© 2019. Published by The Company of Biologists Ltd | Journal of Experimental Biology (2019) 222, jeb200352. doi:10.1242/jeb.200352

RESEARCH ARTICLE

Divergent mechanisms for regulating growth and development after imaginal disc damage in the tobacco hornworm, *Manduca sexta*

Manuel A. Rosero[1], Benedict Abdon[1], Nicholas J. Silva[1], Brenda Cisneros Larios[1], Jhony A. Zavaleta[1], Tigran Makunts[1], Ernest S. Chang[2], S. Janna Bashar[1], Louie S. Ramos[1], Christopher A. Moffatt[1] and Megumi Fuse[1,*]

ABSTRACT

Holometabolous insects have been able to radiate to vast ecological niches as adults through the evolution of adult-specific structures such as wings, antennae and eyes. These structures arise from imaginal discs that show regenerative capacity when damaged. During imaginal disc regeneration, development has been shown to be delayed in the fruit fly *Drosophila melanogaster*, but how conserved the delay-inducing mechanisms are across holometabolous insects has not been assessed. The goal of this research was to develop the hornworm *Manduca sexta* as an alternative model organism to study such damage-induced mechanisms, with the advantage of a larger hemolymph volume enabling access to the hormonal responses to imaginal disc damage. Upon whole-body X-ray exposure, we noted that the imaginal discs were selectively damaged, as assessed by TUNEL and Acridine Orange stains. Moreover, development was delayed, predominantly at the pupal-to-adult transition, with a concomitant delay in the prepupal ecdysteroid peak. The delays to eclosion were dose dependent, with some ability for repair of damaged tissues. We noted a shift in critical weight, as assessed by the point at which starvation no longer impacted developmental timing, without a change in growth rate, which was uncoupled from juvenile hormone clearance in the body. The developmental profile was different from that of *D. melanogaster*, which suggests species differences may exist in the mechanisms delaying development.

KEY WORDS: Developmental delays, Body size, Growth, Irradiation, X-ray damage

INTRODUCTION

Holometabolous insects have been able to radiate to vast ecological niches as adults owing to the evolution of adult-specific structures such as wings, antennae and eyes. These structures arise from imaginal discs – progenitor organs consisting of clusters of epithelial cells at the mesoderm – which differentiate into specific adult structures. In *Drosophila melanogaster*, these discs have been shown to have remarkable regenerative capacity after damage (Bryant, 1971; Bryant and Fraser, 1988; Halme et al., 2010; Schubiger, 1971; Simpson et al., 1980). A variety of damage and ablation experiments have demonstrated the importance of these discs to the coupling of growth and metamorphosis when injury results in a developmental delay. These delays presumably provide sufficient time for tissue regeneration. Injury to imaginal discs has also been shown to delay development in a variety of holometabolous insects, whether through genetic tissue ablation (Colombani et al., 2012; Hackney et al., 2012), surgical ablation or autotomy (Kunkel, 1977; O'Farrell and Stock, 1953, 1954; Stock and O'Farrell, 1954), or X-ray-induced selective damage (Ely and Jungreis, 1977; O'Brien and Wolf, 1964; Poodry and Woods, 1990; Stieper et al., 2008). A delay to allow growth of appropriate adult proportions and healthy adult organs would ensure the success of holometabolous insects in their new niches.

Development in holometabolous insects depends on tight coordination between three major hormones: juvenile hormone (JH), prothoracicotropic hormone (PTTH) and ecdysone. PTTH and ecdysone drive the larval molts in the presence of JH. During the last larval stage, cessation and clearing of JH is required for the release of PTTH and, subsequently ecdysone, to allow pupation to occur (Nijhout, 2015; Nijhout and Williams, 1974b). Timing of JH cessation during the last larval stage has been linked to a nutrition-dependent developmental milestone called critical weight (Nijhout and Williams, 1974b). The critical weight, defined as the mass at which starvation no longer affects developmental timing under normal conditions (Nijhout and Williams, 1974a), delineates the end of nutrition-dependent development and marks the beginning of the terminal growth period prior to wandering and pupation (Fig. 1). At this point, lack of nutrition can affect growth, but does not affect developmental timing. Altogether, these physiological markers have been used as tools to understand how stress affects the growth and development of an individual (Davidowitz et al., 2016).

Disturbance of imaginal disc homeostasis, by means of damage, is a form of stress that has been suggested to disrupt hormone regulation of developmental timing and growth. In *D. melanogaster*, X-ray-induced imaginal disc damage delays pupariation by slowing the larval growth rate (Stieper et al., 2008) and shifting the pre-pupal ecdysteroid peak (Hackney et al., 2012). This change in growth rate is also reflected as an increased critical weight in response to imaginal disc damage (Stieper et al., 2008). The increase in critical weight results in larvae committing to pupation at a higher mass but, coupled with a slowed growth rate during the terminal growth phase, ensures that adult mass is not affected. The delays are suggested to be due to the secretion of Dilp8 – a peptide in *D. melanogaster* named after the insulin-like peptides – from the damaged wing imaginal discs (Colombani et al., 2012; Garelli et al., 2012), as well as a putative retinoid-like factor (Halme et al., 2010). Dilp8 appears to act on both PTTH (Halme et al., 2010; Vallejo et al., 2015) and

[1]Department of Biology, San Francisco State University, 1600 Holloway Avenue, San Francisco, CA 94132, USA. [2]Bodega Marine Laboratory, University of California, Davis, PO Box 247, Bodega Bay, CA 94923, USA.

*Author for correspondence (fuse@sfsu.edu)

M.F., 0000-0001-9245-9465

Received 30 January 2019; Accepted 29 August 2019

Journal of Experimental Biology (2019) 222, jeb200352. doi:10.1242/jeb.200352

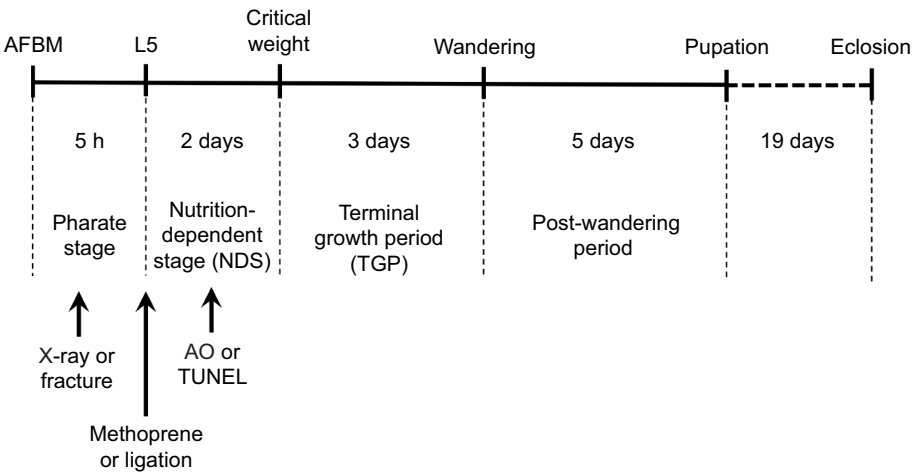

Fig. 1. Schematic of *Manduca sexta* life cycle. Larval *M. sexta* were isolated at the air-filled brown mandible (AFBM) stage as pharate fifth stage animals. Significant developmental stages are noted above and below the timeline (L5, fifth stage at ecdysis). Approximate times for each stage are noted by hours or days below the timeline, and separated by dashed lines. Experimental manipulations are also noted below the timeline with arrows. The dashed line indicates a shortened period. AO, Acridine Orange; TUNEL, terminal deoxynucleotidyl transferase mediated dUTP nick end labeling.

ecdysone signals (Hackney et al., 2012), and the role of retinoids appears to be ecdysteroid independent (Halme et al., 2010). However, the effects of imaginal disc damage are not exclusive to *D. melanogaster*, although similar mechanisms have not yet been elucidated in other models.

We have been developing the tobacco hornworm, *Manduca sexta* (Linnaeus 1763), as a second model organism to study such damage-induced mechanisms. We show that, similar to *D. melanogaster*, *M. sexta* development is delayed after imaginal disc damage with a shift in the pre-pupal ecdysteroid titer. Delays are noted predominantly at the pupal-to-adult transition, in an X-ray dose-dependent manner. However, we find that repair to damaged tissues occurs only when levels of damage are mild, leading to emergence of healthy adults. We also note a shift in critical weight and show that this appears to be uncoupled from JH clearance in the body. We discuss the differences in how development is affected in *M. sexta* and *D. melanogaster* using these data.

MATERIALS AND METHODS

Insect rearing

Larvae of *M. sexta* were raised in individual containers on an artificial wheat germ diet (MP Biomedical, Irvine, CA, USA) under a long-day photoperiod (17 h:7 h light:dark) coupled to a thermoperiod of 27°C:25°C as described by Wells et al. (2006). Pharate fifth instar larvae were staged using external morphological markers, and were treated 1–3 h following brown mandible formation, when the head capsule of the old fourth instar became air-filled [air-filled brown mandible stage (AFBM); see Fig. 1; Copenhaver and Truman, 1982]. AFBM animals typically ecdysed within 4.5±0.4 h (n=50), ensuring that all animals would ecdyse within the same time frame. Larvae were reared individually in their own cups until wandering, at which point they were transferred to wooden blocks without light, to pupate. Afterwards, pupae were transferred to small unsealed plastic bags in larger enclosures, maintained with light and thermal photoperiods.

To track the development of *M. sexta* (Fig. 1), larvae were checked every 24 h after ecdysis to the fifth instar. Animals were kept in cups until they showed wandering behavior, which typically began 5–6 days after ecdysis. Wandering was assessed by (i) presence of frosted frass, (ii) changes in body wall coloration, (iii) presence of extra moisture owing to excess transpiration, (iv) visibility of the aorta on the dorsal side after loss of pigmentation on the overlying epidermis or (v) purging of the gut (Truman and Riddiford, 1974). Upon reaching the wandering stage, the animals were transferred to wooden blocks without light, simulating *M. sexta* burrowing conditions in preparation for pupation. These larvae were monitored for pupation one to two times per day, as noted by peristaltic ecdysis behaviors and removal of the larval cuticle.

Pupae were kept inside the wooden blocks for 17 days, and were removed approximately 2 days before the normal or expected time of adult eclosion. They were placed in individual unsealed plastic bags within large glass tanks, and monitored for adult eclosion one to two times per day. The large enclosures were maintained with light and thermal photoperiods to allow for proper adult eclosion, which was first noted by peristaltic ecdysis behaviors in the abdomen and cracking of the pupal cuticle in the mid-body region. Once emerged, adults were allowed to perch on the glass sides of the tanks to allow proper wing and body expansion as the cuticle hardened. No pupae emerged prematurely in blocks.

Whole-body irradiation

AFBM larvae were exposed to systemic ionizing irradiation using Faxitron 43855A machines (Faxitron Bioptics LLC, Tucson, AZ, USA) operating at 105 kV and 3.0 mA, delivering a dose of 1.5 Gy min^{-1}, with exceptions. Faxitron RX-650 was used for Acridine Orange labeling and for ecdysteroid sampling, operating at 130 kV and 5.0 mA, delivering a dose of ∼10 Gy min^{-1}. Faxitron TRX5200 was used for TUNEL staining, operating at 125 kV and 3.0 mA, delivering a dose of 1.2 Gy min^{-1}. The larvae were irradiated for sufficient lengths of time to produce total exposures of 20–150 Gy, depending on the experiment. Control larvae were placed on top of the Faxitron machines during irradiation in order to control for temperature shifts in the room, as well as vibrations from the machine. After irradiation, all animals were maintained in the regulated light and thermoperiods described above.

Mechanically induced damage to wing imaginal discs

To assess the effects of mechanical damage to the wing imaginal discs (the only discs visible through the body wall), AFBM larvae were randomly sorted into treatment groups. Larvae had their cuticle sterilized with 70% ethanol. Fine forceps were then used to fracture one, two, three or four wing imaginal discs, as described for *D. melanogaster* (Pastor-Pareja et al., 2008). Treatments consisted of no pinch (untreated), sham fractures to the body wall next to the wing imaginal discs, or one to four wing imaginal disc fractures. One fracture consisted of five pinches with forceps, directly onto the wing imaginal disc tissue that was visible through the cuticle to ensure sufficient disc damage. Thus, four disc fractures in a single

Journal of Experimental Biology (2019) 222, jeb200352. doi:10.1242/jeb.200352

animal consisted of 20 consecutive pinches, with shams receiving the same number of pinches to the body wall, without damage to the wing imaginal disc tissue (5 to 20 pinches). Damage to wing discs after fracturing was verified by surgically removing the discs and assessing integrity under a dissecting microscope (data not shown). Larvae that bled or had their cuticle ruptured were not used.

Acridine Orange labeling and scoring

To assess the specificity of irradiation to the imaginal discs, AFBM larvae were irradiated for 6 min (~60 Gy) with the Faxitron RX-650, or maintained as controls. At 24 or 48 h post-irradiation (Fig. 1), larvae were anesthetized on ice, then imaginal discs and brains were quickly dissected in chilled *Manduca* saline (Riddiford et al., 1979) and immediately transferred to microfuge tubes containing a 1 µg ml^{-1} solution of Acridine Orange (Sigma Chemical Co., St Louis, MO, USA). Acridine Orange is a fluorescent dye that accumulates in lysosomes during the condensation of apoptotic corpses, and has been used to detect apoptosis in unfixed tissues of *D. melanogaster* and *M. sexta* (Arama and Steller, 2006; Tanaka and Truman, 2005). Tissues were processed using a modified protocol from Tanaka and Truman (2005). In brief, tissues were incubated for 10 min at room temperature, followed by three quick rinses with 1× phosphate-buffered saline (PBS), pH 7.2. Discs were then viewed as wet mounts in saline on a covered microscope slide. Fluorescent images were taken using a NIKON microscope (Eclipse E600, Nikon Instruments Inc., Melville, NY, USA), and full disc images were created from composite images, using Adobe Photoshop (Adobe Inc., San Jose, CA, USA).

Each tissue was assessed for damage using a rubric of Acridine Orange stain, ranging from 0 to 5, from three independent observers blind to the treatment group of the samples they were assessing. Tissues with the most stain were provided as a metric for maximal scoring and all tissues were graded from 0 (no fluorescence) to 5 (maximal fluorescence). The three independent scores were averaged to provide a single value for each sample. Values never differed by more than a score of 1 between individuals.

TUNEL

To confirm the results obtained from Acridine Orange staining and further assess the specificity of irradiation to the imaginal discs, AFBM larvae were irradiated for 50 min (~60 Gy) with the Faxitron RX5200, or maintained as controls (0 Gy). At 12 h post-irradiation, larvae were anesthetized on ice for approximately 10–15 min, then forewing imaginal discs and brains were quickly dissected in chilled *Manduca* saline (Riddiford et al., 1979). TUNEL (terminal deoxynucleotidyl transferase mediated dUTP nick end labeling) was performed from a composite protocol (Halme et al., 2010; Tanaka and Truman, 2005). Tissues were fixed in 3.7% formaldehyde in PBS for 1 h at room temperature followed by three rinses in PBS at 30-min intervals. Samples were then incubated in 20 µg ml^{-1} proteinase K in 10 mmol l^{-1} Tris, pH 7.5 for 1 h at 37°C and the reaction was stopped by washing three times in PBS-TX followed by three washes at 30 min intervals in PBS. Tissues were rinsed three times in 10 mmol l^{-1} Tris, pH 7.5, and processed with a TUNEL reaction for 1 h at 37°C using the In Situ Death Detection Kit Fluorescein-Texas Red (Roche Applied Science, Indianapolis, IN, USA). Samples were rinsed and washed three times at intervals of 10 min with PBS. The specimens were mounted in glycerol.

Ecdysteroid titers

Manduca sexta hemolymph was collected by cutting an opening in one of the mid-body prolegs and allowing the hemolymph to drain onto a sterilized parafilm strip. For each animal, a 100 µl volume was quickly pipetted into a centrifuge tube containing 300 µl of methanol, and vortexed. Samples were maintained at −20°C until processed. Hormone titers of ecdysteroids were quantified by an enzyme-linked immunosorbent assay (ELISA) as previously described in detail for crustaceans (Abuhagr et al., 2014). The 20-hydroxyecdysone/horseradish peroxidase (20HE-HRP) conjugate and 20-hydroxyecdysone (20HE) antibody were obtained from Dr Timothy Kingan (Kingan, 1989). The 20HE-HRP-conjugated reagent {1:64,000 dilution in assay buffer [AB, 25 mmol l^{-1} sodium phosphate, pH 7.5; 150 mmol l^{-1} NaCl; and 1 mmol l^{-1} EDTA disodium dihydrate with 0.1% bovine serum albumin (BSA; 50 µl)]} was added to all wells of a 96-well plate. Rabbit anti-20HE primary antibody (50 µl; 1:100,000 dilution in AB with 0.1% BSA) was added to all wells, except for the first two wells, which contained only AB plus 0.1% BSA.

Critical weight determination

Critical weight was determined for healthy control animals and irradiated experimental animals by the method described by Helm and Davidowitz (2015). Briefly, non-irradiated animals were selected at the AFBM stage and allowed to feed *ad libitum*. Larvae were then grouped in 0.5 g mass bins (e.g. groups of 1.0–1.4 or 1.5–1.9 g) and separated in two treatment groups, fed and starved. Fed animals were provided sufficient food at all times, while starved animals were restricted to a small piece of polyacrylamide water crystal to prevent dehydration. Starved animals were moved to a clean cup with a new piece of water crystal every other day to prevent infections or drowning. Animals were monitored every 24 h until they reached the wandering stage. Irradiated animals (50 min, or ~75 Gy with Faxitron 43855A) were treated in a similar manner, with both fed and starved groups.

Critical weight was defined as the mass category in which no significant difference was observed for the time to wandering between fed and starved animals (Nijhout and Williams, 1974a). Significance between fed and starved animals was determined by performing a Student's *t*-test for each of the mass bins.

Kr-h1 expression measurement and RT-qPCR analysis

Total RNA was extracted from tissues at AFBM prior to irradiation and then from both healthy controls and irradiated *M. sexta* larvae ~0–2 h after L5 ecdysis, and every 24 h after that for 4 days (prior to wandering). The tissues included a combination of wing imaginal discs, brain, subesophageal ganglion and a total length of three dorsal ganglia, prothoracic glands, gut, fat body, trachea and thoracic muscle. All tissues collected amounted to approximately 30–40 mg of tissue per animal. The tissues were collected by dissecting the larvae in modified Weever's saline (Trimmer and Weeks, 1989), and immediately submerged in 600 µl of RNA-later (Thermo Fisher Scientific, Waltham, MA, USA). Dissected tissues were stored overnight at 4°C, then transferred to a −20°C freezer, where they were stored until the RNA extraction process.

Total RNA was extracted using the RNeasy Mini Kit (QUIAGEN, Germantown, MD, USA) following the methods described in the RNeasy Mini Handbook (2012) for animal tissues. However, one extra step was added: after the first wash with 350 µl RW1 buffer, 10 units of RQ1 RNase-Free DNase (Promega, Madison, WI, USA) were added to the spin column and allowed to incubate at room temperature for 10 min. The DNase was washed away with a second wash of 350 µl RW1 buffer. This extra step was added to ensure that the final product was pure RNA without any DNA contamination. Lastly, the RNA was eluted with nuclease-free water and stored at −20°C.

The expression levels of the JH downstream gene, *Kr-h1*, were measured using the comparative C_t method. *RpL3* was used as an internal reference gene. No significant effects of the time (F=1.094, P=0.298) or dose (F=1.959, P=0.093) in *RpL3* expression levels were noted, nor was any significant interaction between these effects (time×dose, F=0.494, P=0.780), as assessed by two-way ANOVA. *RpL3* was amplified using the same primers used by Koyama et al. (2008): GAGGATAAAGTAAAGTGGGCCAGGG as the forward primer, and CACGCGCAACGACTTTCTCAAAGTG as the reverse primer. It is worth noting that the protein-coding region of *Kr-h1* is not well characterized in *M. sexta*. Therefore, we designed our primers within an area that is highly similar (>80%) to the exon-1 region of the better characterized *Bombyx mori Kr-h1*. The primers used to amplify *Kr-h1* were: GGAGAACGCCCATACACCTG as a forward primer, and CCGTAGACTGCATGGACTGC as the reverse primer. Gene expression was quantified using the Luna Universal One-Step RT-qPCR Kit (New England Biolabs Inc., Ipswich, MA, USA). RT-qPCR reactions were performed in an Applied Biosystems 7300 machine (Applied Biosystems, Foster City, CA, USA). The reactions consisted of a final volume of 20 µl, containing 10 µl of the kit's 2X SYBR master mix, 1 µl of reverse transcriptase enzyme, 100 nmol l^{-1} of each primer and 50 ng of template RNA, and RNase-free water was added to complete 20 µl per reaction. The cycling settings consisted of a holding stage at 55°C for 10 min, then another holding stage at 95°C for 1 min, followed by 40 cycles of 95°C for 15 s and 60°C for 60 s. In addition, specificity of the PCR product was assessed by a melting curve analysis from 60°C to 95°C. Each sample was run in technical triplicates and the mean C_t value of each technical triplicate was transformed into a relative quantity using the comparative C_t method (Livak and Schmittgen, 2001). As part of this method, we used the average relative expression of samples collected at the AFBM stage as baseline. Thus, our results show relative expression of *Kr-h1* as the fold change in expression compared with untreated animals at the AFBM stage.

Methoprene supplementation

Healthy *M. sexta* were supplemented with a JH analog, methoprene (SPEX CertiPrep, Metuchen, NJ, USA; see Fig. 1), to test whether increased JH activity could trigger developmental delays in healthy animals similar to those caused by irradiation-induced damage. Healthy *M. sexta* were supplemented with methoprene approximately 1 h after they had ecdysed to the fifth larval stage. As a negative control, animals were treated with the vehicle cyclohexane. As a positive control, untreated AFBM animals were irradiated for 50 min (~75 Gy) with Faxitron 43855A and monitored. Animals were supplemented with three different doses of methoprene: 0.01, 0.1 and 1 µg. The diluted methoprene was added topically to the dorsal side of unanesthetized animals. After treatment, larvae were placed in individual plastic cups with food *ad libitum*, and their development was tracked as described above.

Ligations

Healthy and irradiated animals (75 Gy, Faxitron 43855A) were ligated slightly posterior to the subesophageal ganglion, but not beyond the first spiracle, where the prothoracic gland is located, thus separating the brain/CC/CA complex from the prothoracic glands. Animals were ligated approximately 1 h after ecdysing to the fifth larval stage, or approximately 6 h after irradiation (Fig. 1). Larvae were ligated for only 24 h after ecdysis because by 48 h only 59% had survived (data not shown), likely due to starvation and hypoxia of the head capsule. After the ligation period, ligatures were carefully cut and the larvae were placed in individual plastic cups with food *ad libitum* and their development tracked as described above.

RESULTS

Development is delayed after tissue damage

To determine whether *M. sexta* responded to tissue damage with delays in metamorphosis and critical weight, as seen in *D. melanogaster*, imaginal discs of pharate fifth instar larvae were damaged and development was timed. Larvae were irradiated at three increasing X-ray doses (Fig. 2) or had discs damaged mechanically (Fig. 3, Fig. S1). The times to begin wandering, pupating and eclosing were monitored. After irradiation, the time to wander was not affected at any X-ray dose (Fig. 2A). In contrast, both the 50 and 75 Gy doses of irradiation induced 0.5–1 day delays in pupation (Fig. 2B), while all doses delayed eclosion, anywhere from 0.5 to 3 days (Fig. 2C, Fig. S4C).

Mechanical damage of one to four wing imaginal discs (Fig. 3, Fig. S1) did not alter the timing to wander (Fig. 3A) or pupate (Fig. 3B), but produced a small delay in the timing of eclosion (Fig. 3C). Eclosion appeared to be delayed by just over a day after damage to any number of imaginal wing discs. Damage to only two or four discs are shown in Fig. 3 for clarity, while damage to one or three discs are shown in Fig. S1. Results were identical for all situations. To control for possible effects of damage to the cuticle owing to pinching, we used shams, where the cuticle next to the imaginal discs was pinched, but no disc was damaged. No differences in development were noted for 5 to 20 pinch shams (data not shown), and thus 20 pinch sham controls are presented in the figures.

Imaginal discs are damaged by X-ray irradiation

We verified imaginal disc damage produced by whole-body X-ray irradiation by noting phenotypic abnormalities in pupal and adult structures arising from the irradiated discs (Fig. S2), and by assessing and quantifying cell damage/death in the imaginal discs (Fig. 4, Fig. S3). Imaginal discs were clearly damaged upon irradiation, as noted by damage to wings, antennae and eye regions (data not shown) in the pupae (Fig. S2C,D, arrowheads and arrows, respectively) compared with controls (Fig. S2A,B). In most cases, adults showed complete recovery to low doses of irradiation (data not shown), but only marginal repair to these areas after high irradiation doses (Fig. S2D) compared with controls (Fig. S2B).

We also assessed the level of damage at the cellular level in wing imaginal discs. Wing imaginal disc cells in *M. sexta* proliferate continuously and exponentially throughout the late larval and pre-pupal periods (Nijhout et al., 2014), suggesting they should be vulnerable to irradiation. To assess the specificity of damage by whole-body X-ray irradiation, wing imaginal discs from irradiated larvae were dissected and compared with control discs (Fig. 4, Fig. S3, Table 1). Wing discs showed significant increases in Acridine Orange stain (Fig. 4, Table 1) and in TUNEL staining (Fig. S3) after whole-body irradiation, while no significant stain was noted in the brains. Acridine Orange stain was noted in irradiated forewing and hindwing imaginal discs 24 and 48 h after irradiation (Fig. 4C,D,G,H, respectively), but not in controls (Fig. 4A,B,E,F). Brains of non-irradiated and irradiated animals showed no stain (Fig. 4I–L). Blinded scoring of stain intensity, on a scale of 1 to 5, revealed significant differences in this stain intensity in imaginal discs after X-ray compared with their control counterparts (P<0.05; Table 1). The TUNEL assay revealed apoptosis as early as 12 h after irradiation compared with control discs (Fig. S3A,C) and minimal label was noted in non-irradiated and irradiated brains (Fig. S3B,D).

Journal of Experimental Biology (2019) 222, jeb200352. doi:10.1242/jeb.200352

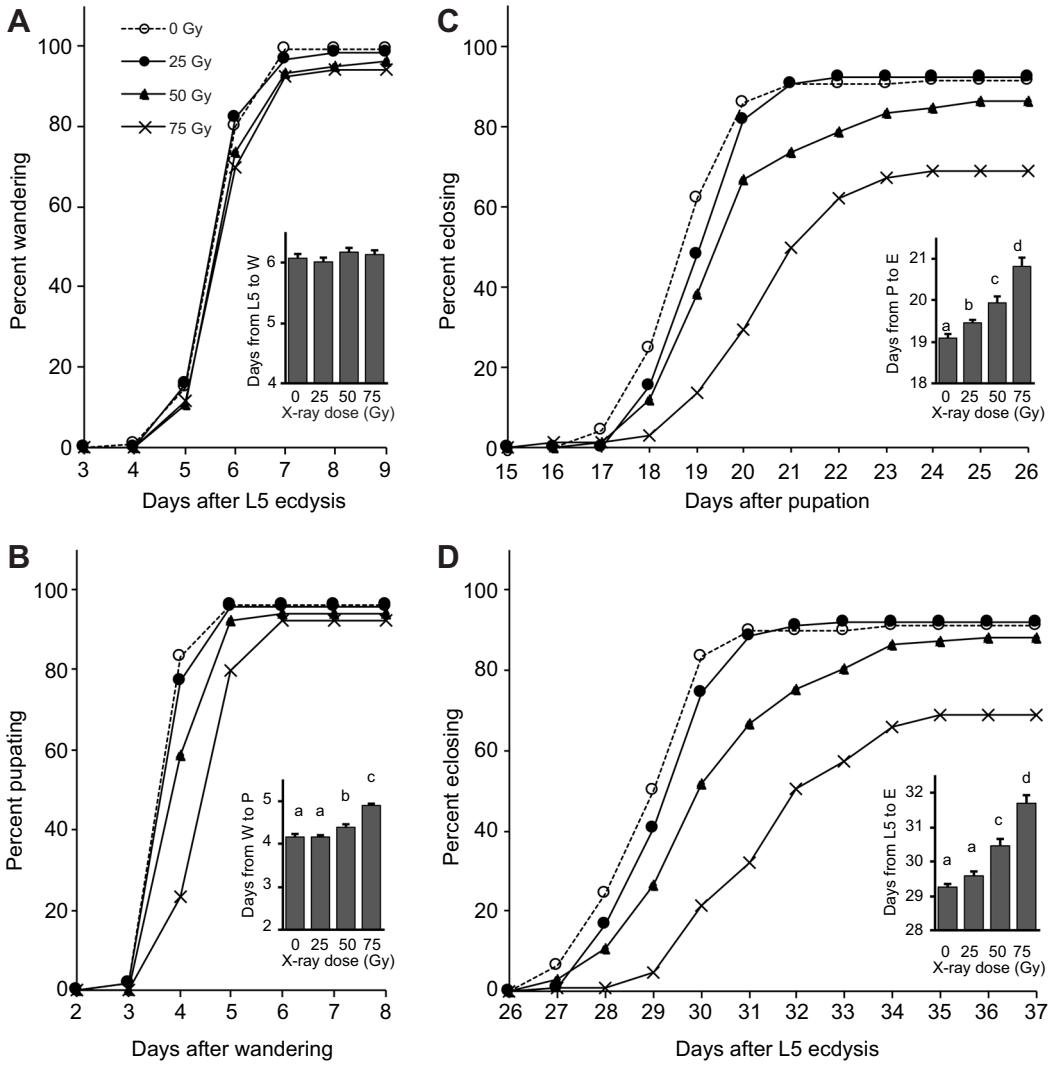

Fig. 2. Developmental timing is delayed after irradiation. Pharate fifth stage *M. sexta* larvae were irradiated at three doses: 25 Gy (n=108), 50 Gy (n=96) and 75 Gy (n=95). Development was monitored and compared with controls at 0 Gy (n=122). The percentage of animals were timed from (A) irradiation to wandering, (B) wandering to pupation, (C) pupation to eclosion and (D) irradiation to eclosion. Insets represent average times with s.e.m. Letters represent significant differences from each other, as assessed by one-way ANOVA with pairwise t-tests corrected by the Holm–Šidák method for multiple comparisons (P<0.05).

Ecdysteroid titer is shifted proportional to developmental delays after irradiation

In order to determine whether pre-pupal ecdysteroid titers were altered after X-ray irradiation, as has been noted in *D. melanogaster* (Hackney et al., 2012), ecdysteroid levels were quantified by ELISA (Fig. 5). Hemolymph from larvae irradiated just prior to L5 ecdysis was collected every 12 h after larvae reached the wandering stage. The ecdysteroid titer of control (0 Gy) larvae peaked around day 2 after larvae started wandering, then declined by day 4 just prior to pupation. In contrast, the ecdysteroid titer of irradiated larvae (75 Gy) peaked ∼1.5 days later than control larvae and had not fully declined by day 4. Sample sizes were lower at the beginning and end of the titers, owing to values often being below the detection level of our assay.

Critical weight is increased after irradiation, but growth rate is not altered

Critical weight has been shown to shift after X-ray-induced imaginal disc damage in *D. melanogaster* (Stieper et al., 2008). To determine whether the same phenomenon occurred in *M. sexta*, the critical weight was assessed after significant X-ray damage (Fig. 6). Under control conditions (non-irradiated), the critical weight was determined to be approximately 5.5 g because, after reaching this mass, starvation no longer delayed development (Fig. 6A). In contrast, irradiated animals showed an increased critical weight of approximately 7.5 g (Fig. 6B).

The growth rate of these larvae was also assessed, as the daily wet mass of each animal (Fig. 6C). The growth rate of *M. sexta* was not affected by irradiation. There were no significant daily differences in mass (P>0.5), even at the peak mass of approximately 12.0 g. Both groups attained their final body size on the same day at wandering.

JH activity is not altered after irradiation

Critical weight has been considered a proxy for JH levels in *M. sexta* (Davidowitz, 2016; Nijhout and Williams, 1974b). To determine whether the delay in pupal commitment associated with the irradiation-induced increase in critical weight was also

Journal of Experimental Biology (2019) 222, jeb200352. doi:10.1242/jeb.200352

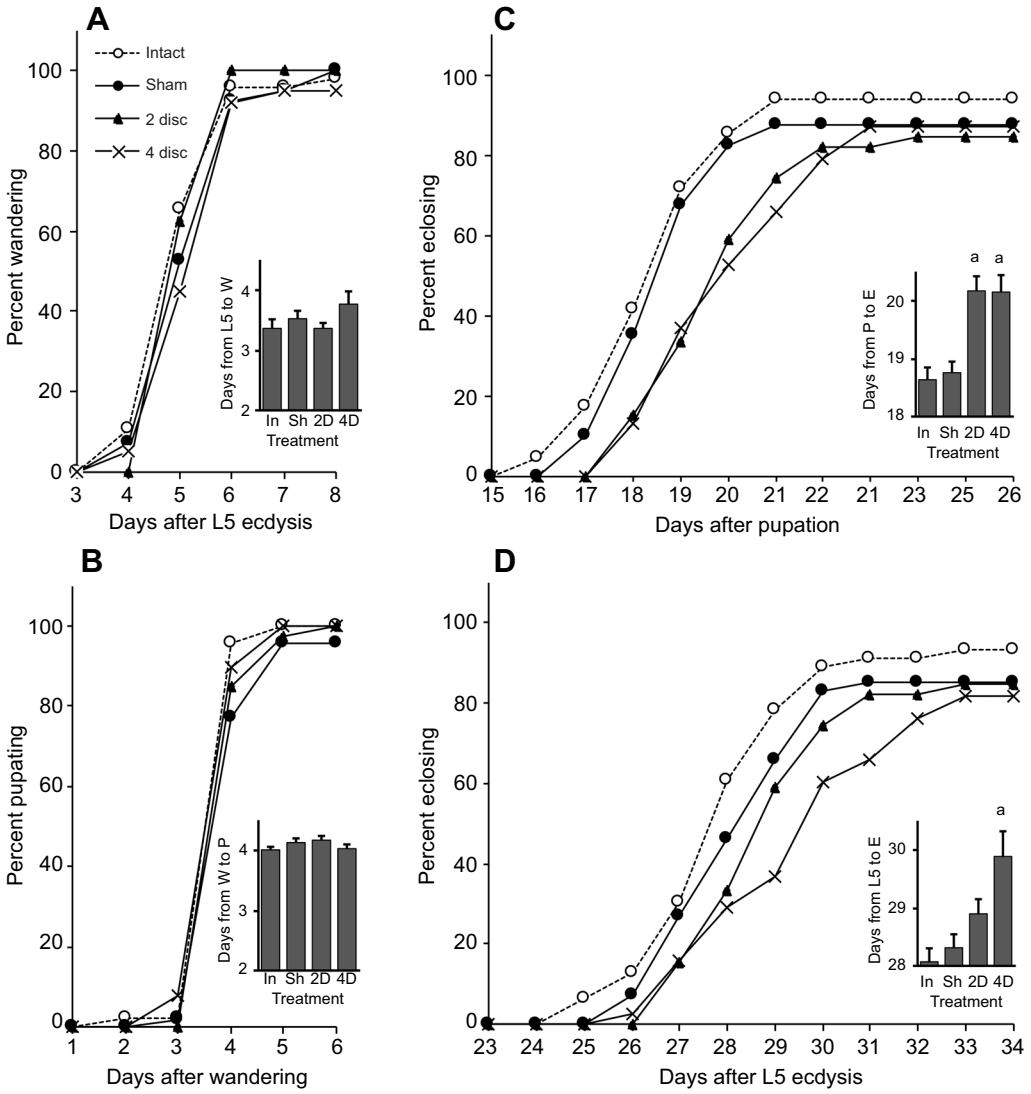

Fig. 3. Developmental timing is only moderately delayed after mechanical damage to wing imaginal discs. Two wing (2D; *n*=41) or four wing (4D; *n*=38) imaginal discs were mechanically damaged in pharate fifth stage *M. sexta* larvae and were compared with intact (In; *n*=56) or four disc sham (Sh; *n*=38) controls. Other fractures and controls are in Fig. S1. The percentage of animals were timed from (A) fracture to wandering, (B) wandering to pupation, (C) pupation to eclosion and (D) fracture to eclosion. Insets represent average times with s.e.m. Letters represent significant differences from each other, as assessed by one-way ANOVA with pairwise *t*-tests corrected by the Holm–Šidák method for multiple comparisons ($P<0.05$).

accompanied by a delay in the decline of JH levels, we assessed whether JH levels shifted proportionally to the delayed critical weight after X-ray irradiation. We measured changes in transcription levels of the downstream signal of JH activity, Krüppel Homolog 1 (*Kr-h1*). *Kr-h1* transcription has been used as an indicator of JH activation of its putative receptor, Methoprene-tolerant (Met; Kayukawa et al., 2014; Lee et al., 2015; Minakuchi et al., 2007, 2009). Starting levels of *Kr-h1* at AFBM were consistently low, with little variation between animals. As expected, there was a marked increase in transcription of *Kr-h1* mRNA around the time of ecdysis to L5, followed by a return to pre-ecdysis levels over the next 72 h (Fig. 7). Notably, there were no significant differences in *Kr-h1* mRNA expression between control and irradiated larvae, which were assessed over 4 days at 12 h intervals from the beginning of L5 ecdysis, despite the shift in critical weight.

Head ligation partially rescues X-ray-induced developmental delays

To confirm our observations of *Kr-h1* expression, we tested whether a simple increase in JH levels could result in developmental delays such as those observed as a result of irradiation-induced tissue damage. Supplementation with the JH analog, methoprene, early in the last larval instar did not cause statistically significant changes in time to wandering (Fig. S4A), pupation (Fig. S4B) or eclosion (Fig. S4C). But, as expected, radiation treatment without methoprene did cause delays to pupation and eclosion (Fig. S4B and C, respectively).

We further reasoned that if JH played a role in the damage-induced developmental delays, then removal of JH would rescue normal developmental timing in damaged animals. To test this idea, animals were ligated posterior to the brain/CC/CA complex, but anterior to the prothoracic glands (Fig. 8D–F). This prevented JH from being released into the body, where tissues such as the prothoracic glands, the primary source of ecdysone, were located. Ligations are known to prevent flow of hormones from their source gland to the rest of the body (Hatakoshi et al., 1988; Suzuki et al., 2013; Truman et al., 2006). Larvae were ligated for only 24 h after ecdysis because during that period of time JH activity is at its highest, thus preventing JH from reaching the rest of the body when it was most active. The absence of JH in the body (as well as anterior ganglia including brain and subesophageal ganglion), through ligations, only partially rescued developmental timing in irradiated larvae. That is, ligations partially prevented irradiation-induced delays to pupation (Fig. 8B) by approximately half a day, and fully rescued adult eclosion (Fig. 8C). It should be noted that, although not significant, there was a trend towards a mild increase in developmental timing of adult eclosion after irradiation and ligation, as was noted in pupae. Interestingly, ligated animals wandered ~7 days after ecdysis whether irradiated or not, compared with non-ligated larvae, which wandered on day 6 (Fig. 8A).

Journal of Experimental Biology (2019) 222, jeb200352. doi:10.1242/jeb.200352

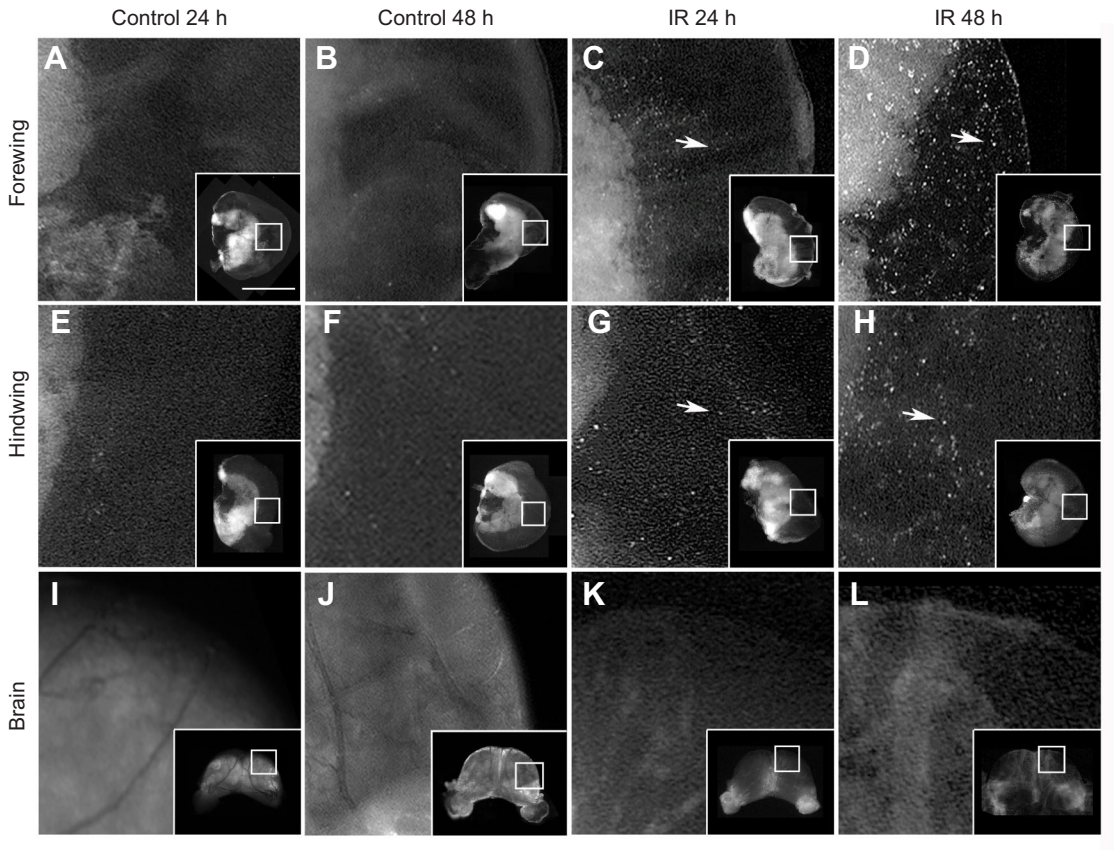

Fig. 4. Acridine Orange stain is elevated in wing imaginal discs but not brains after irradiation. Wing imaginal discs and brains were stained with acridine orange (AO) after X-ray irradiation at the pharate fifth larval stage. Control forewing and hindwing discs as well as brains were stained at 24 h (A,E,I) and 48 h (B,F,J). Similar tissues were dissected and stained at 24 h (C,G,K) and 48 h (D,H,L) after irradiation at 60 Gy. Arrows point to examples of accumulated AO stain. Whole tissues are represented in the smaller inset. The larger image represents a magnified section of the area outlined by the boxed region of the whole tissue. All images are composites of four to six original images compiled with Adobe Photoshop. The scale bar noted in A represents 600 µm for all smaller inset images and 60 µm for all large images.

We confirmed the efficacy of ligations by measuring *Kr-h1* expression in tissues collected from ligated animals. As we expected, tissues collected from ligated animals showed a significant decrease in expression of *Kr-h1* (data not shown), which confirmed that ligations prevented the flow of JH from the CA to the rest of the body.

DISCUSSION

Delays in development appear to be a conserved response to imaginal disc damage in holometabolous insects

We show that the holometabolous insect *M. sexta* can be used as a model to study the regulation of growth and development after selective imaginal disc damage when whole-body X-ray irradiation is used to directly damage imaginal discs (Fig. 2) or when discs are fractured manually (Fig. 3). Even though we only compared wing imaginal disc damage with that of brains after whole-body irradiation to verify selective damage of the discs (Fig. 4, Fig. S3), other tissues such as the gut, salivary glands, lymph glands and fat tissue have likewise been shown to be unaffected by irradiation in *D. melanogaster* when wing discs are damaged, using both TUNEL and caspase staining methods (Halme et al., 2010). The extent of damage to imaginal discs appears to go beyond the wings because other discs such as eyes (data not shown) and antennae also appeared damaged in *M. sexta*, as noted phenotypically (Fig. S2). Thus, whole-body irradiation appears to be an effective strategy for studying the developmental effects of imaginal disc damage in this newer, larger insect model.

Table 1. Score of Acridine Orange stain

	24 h (control)	24 h (irradiated)	48 h (control)	48 h (irradiated)
Forewing	1.3±0.3 (11)	4.1±0.2 (7)*	0.3±0.4 (3)	3.8±0.3 (11)*
Hindwing	1±0.2 (10)	3.6±0.4 (7)*	1.2±0.4 (3)	3.9±0.3 (10)*
Brain	0.1±0.1 (7)	0.1±0.1 (6)	0.2±0.2 (3)	0.1±0.1 (8)

Subjective double blind scoring of stain in imaginal discs and brain tissue. Values are averages with s.e.m., on a scale ranging from 0 to 5 as described in the Materials and Methods. Sample sizes are noted in parentheses. Asterisks represent significant differences from respective controls assessed by Wilcoxon rank sum test (P<0.001).

Imaginal disc damage after whole-body irradiation in *M. sexta* resulted in delays in the pupal and adult stages similar to those seen for *D. melanogaster* after whole-body irradiation (Halme et al., 2010; Stieper et al., 2008) and after genetically induced imaginal disc damage (Colombani et al., 2012; Hackney et al., 2012). Delays have also been described in other insects after injury (Bourgin et al., 1956; Bryant and Simpson, 1984; Ely and Jungreis, 1977; Halme et al., 2010), suggesting that the developmental delay response to imaginal disc damage may be conserved amongst insects.

The developmental delays noted at pupation and eclosion in irradiated *M. sexta* indicate that both the larval and pupal stages are extended after imaginal disc damage (Figs 2 and 3). Presumably,

Journal of Experimental Biology (2019) 222, jeb200352. doi:10.1242/jeb.200352

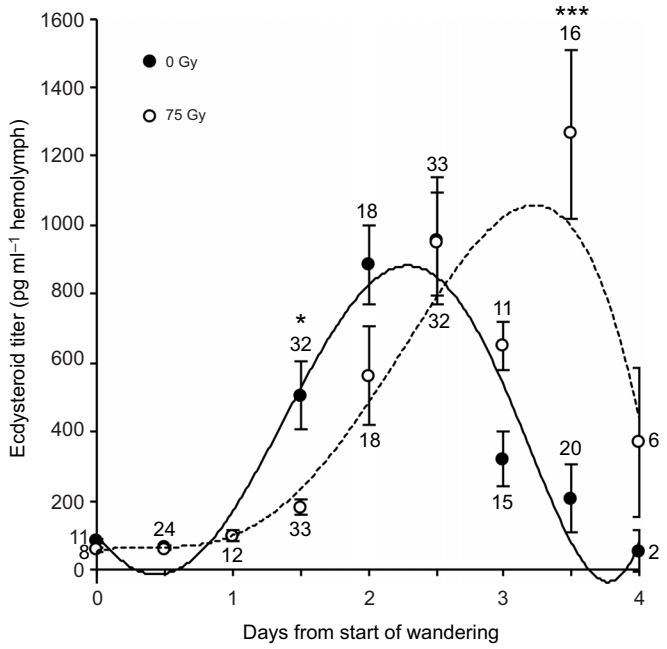

Fig. 5. Ecdysteroid titers are shifted after X-ray irradiation. Hemolymph samples were taken in 12 h increments starting at wandering (day 0), after X-ray irradiation at the AFBM stage. Data are averages with s.e.m. Sample sizes are noted next to each data point, and where only one sample size is noted, values were identical between controls and X-rayed animals. Asterisks represent statistically significant differences between the control and irradiated groups, as determined by a two-way ANOVA with *post hoc* Student's *t*-tests corrected by the Holm–Šidák method for multiple comparisons (*P=0.06; ***P<0.0001).

these delays provide an extended developmental window for growth plasticity while imaginal discs regenerate before development continues (Madhavan and Schneiderman, 1969; Jaszczak et al., 2015; Boulan et al., 2019). This response appears to be dose dependent: greater damage by irradiation produces longer delays (Fig. 2). This may reflect secretion of delay factors by the damaged discs, where greater damage results in greater secretion. In contrast, we noted that there were only limited delays after selective mechanical damage to just the wing imaginal discs. That is, only eclosion was delayed, even after damage to four wing discs (Fig. 3, Fig. S1). We suggest that the longer delays after irradiation may have been due to imaginal disc damage beyond just the wings, such as to antennae, proboscis and eyes (Fig. S2). We cannot rule out the possibility that fracturing the wing discs compromised tissue integrity rather than inducing cellular damage such as apoptosis, and as such, different mechanisms may have been at play in delaying eclosion rather than pupation. This seems less likely, given that integumentary mechanical damage to another holometabolous insect, *Galleria melonella*, delayed pupation (Malá et al., 1987). These differences nevertheless merit further investigation, possibly through localized irradiation, by shielding some imaginal discs during the irradiation process. This was done successfully in *D. melanogaster*, where Jaszczak et al. (2015) were able to localize damage to wing imaginal discs.

Although both *M. sexta* and *D. melanogaster* delayed their development in response to imaginal disc damage, they appeared to do so using different mechanisms. In *M. sexta*, we noted the greatest delays during the pupal stage, ranging from 0.5 to 3 days, while the larval stage was typically extended by 1 day. The extension of the larval stage in *M. sexta* was short in comparison to the 3–5 day

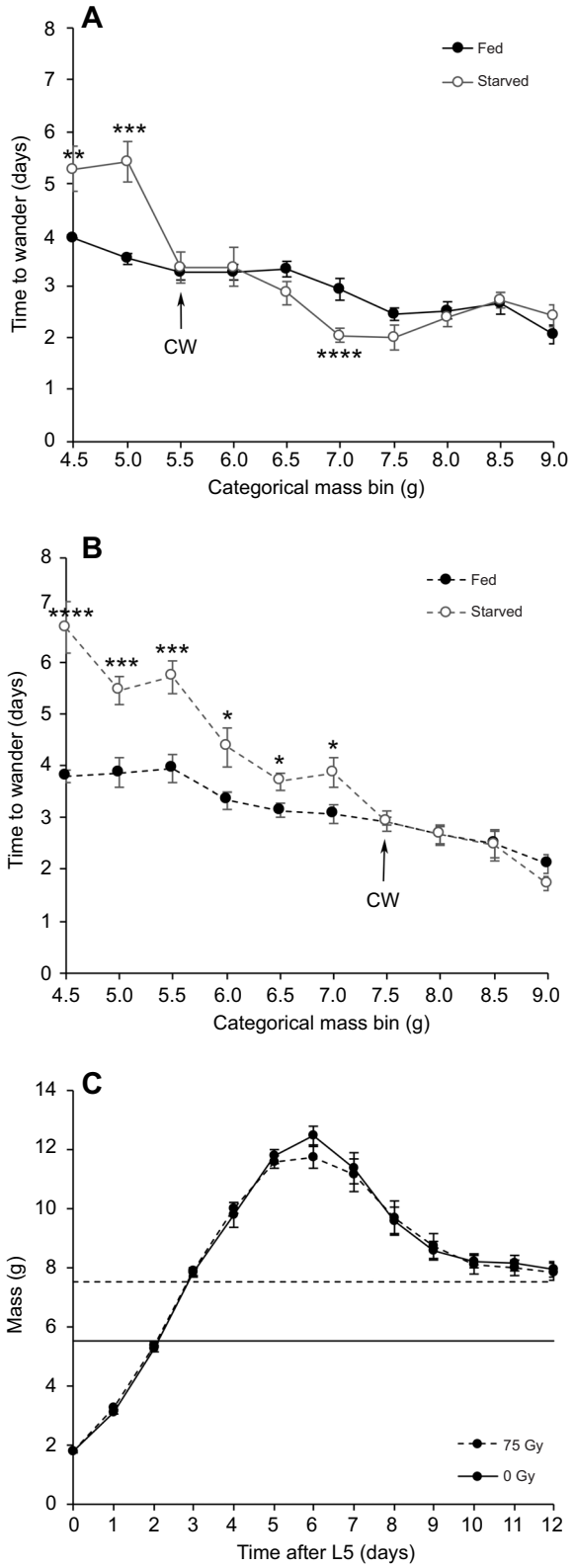

Fig. 6. See next page for legend.

extensions in *Drosophila* larvae after imaginal disc damage (Hackney et al., 2012), especially given the longer life cycle in *M. sexta*. A 2-day delay in *D. melanogaster* comprises approximately 15% of its life cycle in comparison to only 5% in *M. sexta*. Moreover, the extent of repair after damage appeared less in *M. sexta* as well (Fig. S2). A compelling explanation for the less extensive delays in

Journal of Experimental Biology (2019) 222, jeb200352. doi:10.1242/jeb.200352

Fig. 6. Critical weight, but not growth rate, is altered after irradiation. Critical weight is defined as the mass where there is no statistically significant developmental delay due to starvation. Time to wander in fed (black circles) and starved (white circles) conditions was determined for (A) healthy animals at 0 Gy (solid lines) and (B) animals irradiated at 75 Gy (dashed lines). Arrows indicate the critical weight (CW) for each group. Sample sizes were: fed at 0 Gy (n=283) or 75 Gy (n=151), or starved at 0 Gy (n=166) or 75 Gy (n=133). Groups were placed into 0.5 g bins resulting in n=14–20 per bin. Asterisks represent statistically significant differences between the fed and starved groups within the same mass bin, as determined by Student's t-test (*P<0.05; **P<0.01; ***P<0.001; ****P<0.0001). (C) Growth rates of healthy at 0 Gy (solid line) and irradiated at 75 Gy (dashed line) larvae, from the beginning of the fifth instar to pupation, as daily mean±s.e.m. masses (n=26). Critical weight values are taken from A and B and are indicated as horizontal lines on the graph. No statistically significant differences were noted in mass between doses, as determined by a two-way ANOVA (P>0.5).

M. sexta arises from its apparent lack of *Drosophila* insulin-like peptide 8 (Dilp8), a peptide secreted from damaged discs that modulates developmental delays and growth plasticity in *D. melanogaster* (Colombani et al., 2012; Garelli et al., 2012; Jaszczak et al., 2015). The most recent publicly available *M. sexta* genome does not include a sequence representative of Dilp8 (Table S1), which appears to be lacking in other holometabolous insects as well.

Nevertheless, there appear to be conserved mechanisms in place to delay development by delaying the secretion of ecdysone in both *M. sexta* (Fig. 5) and *D. melanogaster* (Hackney et al., 2012; Halme et al., 2010). This suggests that dysregulation of developmental hormones may be a mechanism of action of damaged imaginal discs to delay development and enhance the probability of coordinated adult growth (Boulan et al., 2019). We cannot discount the possibility that a completely unique delaying factor may be secreted from damaged imaginal discs in *M. sexta*. The putative retinoid

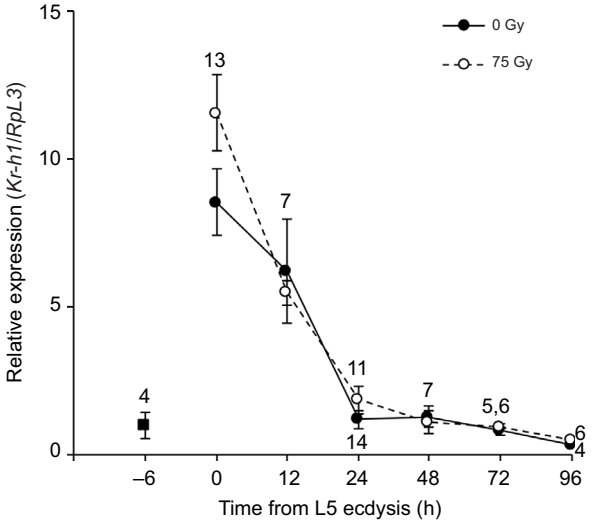

Fig. 7. The pattern of *Kr-h1* expression is not altered after irradiation. The relative transcription levels of *Kr-h1* were measured from controls at 0 Gy (solid line) and irradiated at 75 Gy (dashed line) larvae, normalized to *RpL3* expression. Tissues were assessed 6 h prior to ecdysis (–6) before irradiation (squares), then after irradiation every 12 h from the beginning of the fifth larval instar (circles), for 4 days. Each data point represents the mean±s.e.m. relative expression level. Sample sizes are noted next to each data point, and where only one sample size is noted, values were identical between controls and X-rayed animals. Two-way ANOVA indicated that there were no significant differences between doses (P>0.05), although in both cases, daily levels after ecdysis were significantly higher than the –6 h baseline, until 96 h.

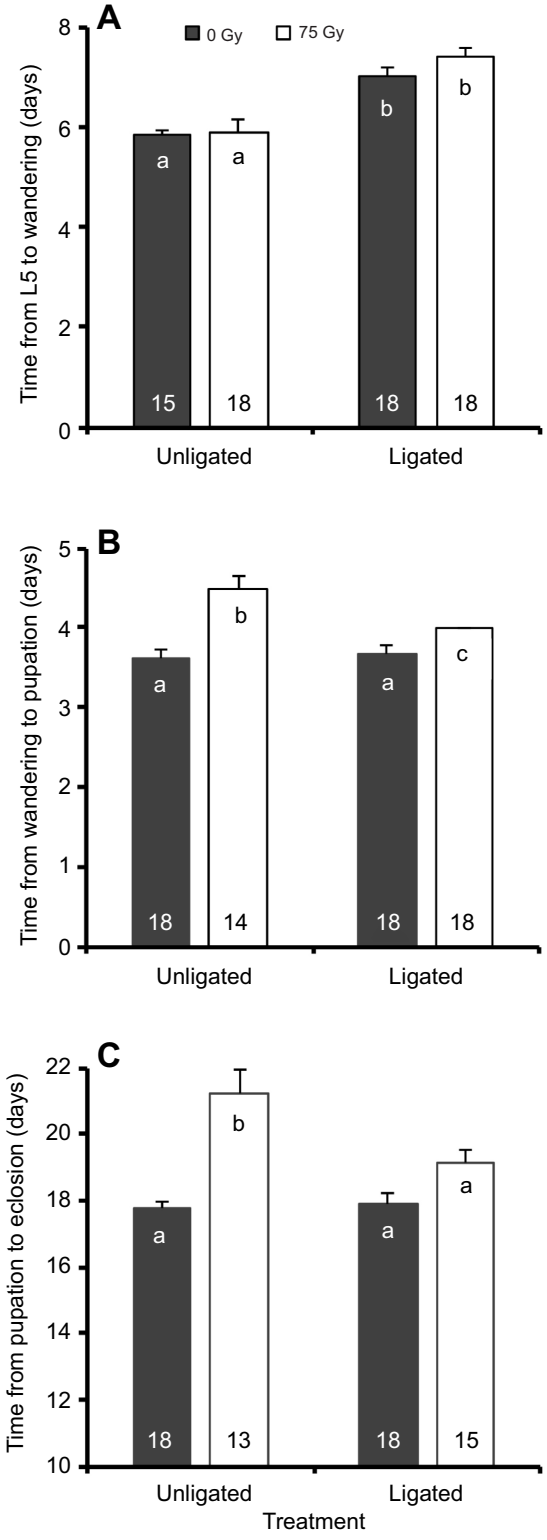

Fig. 8. Ligation partially rescues radiation-induced developmental delays. Development was monitored after irradiation at AFBM (white bars) or in non-irradiated controls (gray bars) with or without ligation. Larvae were ligated posterior to the brain/CC/CA complex for 24 h immediately after ecdysis. Development was tracked for (A) the time to wander relative to fifth instar ecdysis, (B) the time to pupate relative to wandering or (C) the time to eclose relative to pupation. Bars represent means±s.e.m. Sample sizes are noted within the bars. Letters represent significant differences from other groups, as assessed by two-way ANOVA with *post hoc* pairwise t-tests corrected by the Holm–Šidák method for multiple comparisons (P<0.05).

signaling pathway previously suggested to work in *D. melanogaster* (Halme et al., 2010) could very likely still act to regulate developmental timing after imaginal disc damage in *M. sexta*. Thus, there may be multiple secreted factors affecting development, some of which are conserved across species while others are not. It will be important to assess hormone titers at all developmental stages following irradiation to see where the effects are most noted.

JH decline is uncoupled from critical weight after imaginal disc damage

Critical weight is a developmental milestone in fifth instar larvae that has been identified as an endocrine proxy, most specifically to JH levels (Davidowitz, 2016; Nijhout and Williams, 1974b). By definition, critical weight is the point in development when lack of nutrition no longer delays time of PTTH release, required to stimulate the increases in ecdysone in the hemolymph necessary for wandering and pupation (Nijhout and Williams, 1974a). Release of PTTH is dependent on the cessation of JH secretion, which appears to be the critical endocrine event triggered when critical weight is reached, at least under typical conditions. Once JH titers fall, the hormonal cascade that stimulates PTTH release, ultimately causing wandering behaviors and eventually pupation, is initiated (Nijhout and Williams, 1974b). Thus, under normal conditions in *M. sexta*, critical weight is thought to link nutrition-sensing mechanisms, such as insulin signaling, with the cessation of JH, where it ultimately defines developmental timing and final body size (D'Amico et al., 2001; Davidowitz et al., 2003; Hatem et al., 2015; Nijhout and Williams, 1974b). Yet in this system, imaginal disc damage in *M. sexta* increased the critical weight, without significantly altering growth rate, and delayed pupation but not wandering. Moreover, even though critical weight was increased by irradiation, there was apparently no accompanying change in the pattern of JH secretion, as assessed by *Kr-h1* expression levels (Fig. 7). Thus, even though irradiated animals reached their critical weight at a later age than control animals, their JH levels appeared to decline at the same rate and on the same day of development as control animals, and they wandered at the same time. This indicates that JH titers became uncoupled from critical weight after imaginal disc damage, and that the effects of irradiation worked downstream of JH activity.

It will be important to determine the JH levels in *M. sexta* and *D. melanogaster* directly, as comparisons, and what pre-wandering ecdysteroid titers look like. JH activity was assessed by *Kr-h1* expression, thus we cannot discount the possibility that JH titers remained high but were acting through a different receptor pathway than the typical Met receptor. It has been suggested that JH can act on different signaling pathways (Kayukawa and Shinoda, 2015; Wilson and Fabian, 1986; Zhao et al., 2014). For instance, high concentrations of JH have been shown to bind to the orphan receptor Ultraspiracle (Jones et al., 2001), and membrane-bound receptors have been suggested to exist in insect ovaries (reviewed by Davey, 2007). This does not appear likely in our experiments, however, given that ligations, placed posterior to the head capsule to inhibit JH activity in the body, only partially rescued normal developmental timing (Fig. 8). Likewise, supplementation with methoprene did not delay pupation or eclosion (Fig. S4). The doses of methoprene we used did not induce erroneous development, such as supernumerary larval molts or hybrid larval–pupal molts (Hatakoshi et al., 1988). At higher doses, we did note similar larval–pupal hybrid transitions (data not shown). These data therefore suggest that a factor from the head capsule appears to at least partially delay development in irradiated larvae, but what this is remains unclear, given the lack of change in JH signaling in irradiated larvae. It will be important to determine the JH, PTTH and ecdysteroid titers in both *M. sexta* and *D. melanogaster* to determine what roles they all play in the developmental delays noted after imaginal disc damage.

Understanding how damage to imaginal discs affects critical weight in *M. sexta* is an important first step to defining the endocrine signals that may be disrupted after imaginal disc damage, resulting in delayed development. Although a shift in critical weight without any changes in wandering time (Fig. 2B), growth rate (Fig. 6C) or *kr-h1* expression levels (Fig. 7) may warrant caution in regards to the sample size used in this experiment, the effect of food availability on developmental timing had strong statistical power for both healthy and irradiated animals ($\beta<0.1$ for both data sets).

We had expected delays in the onset of wandering following such a large shift in critical weight without a concomitant change in overall growth rate, as was noted in *D. melanogaster* (Stieper et al., 2008). The method we used has been well established in *M. sexta*, but it was not the same method used with *D. melanogaster*. The critical weight of the fly is determined by a bi-segmented linear regression, where the breakpoint represents the critical weight (Stieper et al., 2008). Even using a bi-segmented linear regression in our data set, we observed a shift in critical weight of *M. sexta* (data not shown). These differences in methodology shed light on the inconsistency of critical weight as an endocrine proxy across insect species, highlighting the importance of confirming endocrine inferences through more direct measurements. It will be imperative to assess the pre-wandering ecdysteroid titers, which we assume will not be shifted after irradiation in *M. sexta*, given the lack of delay in wandering. These peaks have not been assessed in *D. melanogaster* either, although pre-pupal shifts have been noted in both *M. sexta* (Fig. 5) and *D. melanogaster* (Hackney et al., 2012), which were accompanied by delays in pupation.

As a side note, there was an interesting significantly faster rate of development in control starved (non-irradiated) animals within the 7.0 g group (Fig. 6A) that has not been previously reported (D'Amico et al., 2001; Davidowitz et al., 2003; Helm and Davidowitz, 2015; Nijhout and Williams, 1974a). This may have been due to overcompensation as a result of the delays by starvation, but requires further investigation.

A model for developmental delays in *M. sexta*: nutrition-sensing mechanisms

The responses in *M. sexta* differ in some ways from changes noted in *D. melanogaster* after irradiation (Stieper et al., 2008; see Fig. 9). In *D. melanogaster*, Dilp8 signaling modulates hormone secretion to serve two different functions: to regulate developmental timing and to coordinate growth of undamaged tissues. Through the modulation of hormone secretion, Dilp8 acts as a delay factor to downregulate the insect's growth rate to delay development (Vallejo et al., 2015), as well as a size sensor to coordinate the growth of healthy tissues as the damaged tissues recover (Jaszczak et al., 2015; Boulan et al., 2019). Together, both mechanisms serve to alter the growth rate and critical weight (Stieper et al., 2008), consequently altering developmental timing in *D. melanogaster*.

We observed a similar shift in critical weight in *M. sexta* (Fig. 6B), but we did not see changes in growth rate (Fig. 6C). This contrast suggests that *M. sexta* regulates developmental timing in response to imaginal disc damage independent of mechanisms that regulate growth. The differences noted between *M. sexta* and *D. melanogaster* indicate that some of the mechanisms uncovered in *D.*

Journal of Experimental Biology (2019) 222, jeb200352. doi:10.1242/jeb.200352

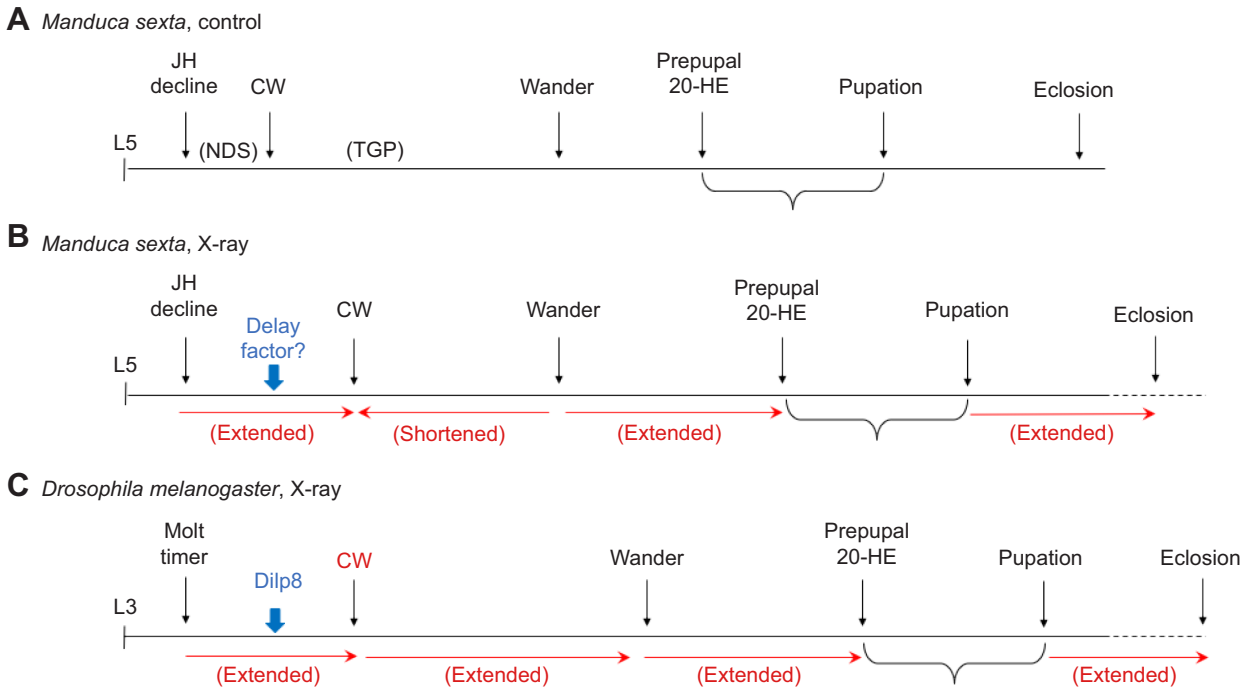

Fig. 9. Model for developmental delays associated with imaginal disc damage. Graph of developmental trajectory for (A) control *M. sexta*, (B) irradiated *M. sexta* and (C) irradiated *Drosophila melanogaster*. Black indicates data that are known. Red indicates changes in timing from controls. Blue indicates hypothetical results. NDS, nutrition-dependent stage; CW, critical weight; TGP, terminal growth period; 20-HE, 20-hydroxyecdysone.

melanogaster are not redundant in *M. sexta*. This could explain the limited delays and regenerative capacity observed in *M. sexta*. These differences may arise from differences in the regulation of growth and development under normal conditions. For instance, in *D. melanogaster*, ecdysteroid biosynthesis depends on coordinated signals from insulin and PTTH, but this does not appear to be the case in *M. sexta* (Mirth et al., 2005; Smith et al., 2014). This suggests that the limitations in the duration of developmental delays in *M. sexta* may arise from differences in regulation of hormone secretion. In addition, *D. melanogaster* and *M. sexta* clearly respond differently to a variety of environmental stresses and hormonal shifts. For instance, *D. melanogaster* goes through premature metamorphosis under starved conditions after attaining critical weight, resulting in smaller adults (Stieper et al., 2008), whereas *M. sexta* shows normal developmental timing, which allows it to maintain a relatively normal body size. Likewise, application of JH in the last larval instar results in a supernumerary molt in *M. sexta* (Cymborowski et al., 1982; Hatakoshi et al., 1988), which is not the case with *D. melanogaster* (Mirth et al., 2014).

Our data provide a model for how regulation of growth and developmental timing varies between *D. melanogaster* and *M. sexta* (Fig. 9). Although both *M. sexta* and *D. melanogaster* showed increased critical weight after X-ray, growth rate only changed in *D. melanogaster*. Increasing critical weight may be a mechanism to ensure enough nutrient storage necessary to satisfy the growth and repair of damaged imaginal discs during the extended developmental period, but the different responses in growth indicate different regulatory mechanisms. For instance, the terminal growth period is delayed in *D. melanogaster*, resulting in a delay to wandering, but is shortened in *M. sexta*, resulting in a constant wandering period, but an extended post-wandering phase prior to pupation. This reduced terminal growth period may also account for the shorter delay noted to pupation in *M. sexta* compared with *D. melanogaster*, relative to the lengths of their life cycles. Thus, it is not entirely surprising that these two insect species respond differently to the same tissue insults. Using *M. sexta* as an alternative model to understand the regulation of growth and development in response to tissue damage may shed light on the evolutionary divergence of mechanisms designed to generate similar physiological responses. Therefore, it would be interesting to expand this investigation to other well-characterized holometabolous insects, such as *B. mori*.

Conclusions

Differences in life history of these two insect species may account for some of the differences in the regulation of growth and development. For example, larval *D. melanogaster* becomes more visible to predators as it pupates, with its dark coloration providing contrast to the lighter medium it rests on. Thus, extending the larval stage during imaginal disc repair for days may be more advantageous than extending the pupal phase to the same extent. In contrast, *M. sexta* pupates below ground, providing optimal cover for an extended pupal developmental period. Whether the delays noted in this study indicate an evolutionary adaptation based on life history strategies may become apparent when we eventually compare delays in a variety of other holometabolous insects.

Developmental delays associated with tissue damage appear to be conserved in many insects and are presumed to be a mechanism to allow time for repair of the damaged imaginal discs. Life histories of different insects may dictate where the majority of the delays occur – at the larval or pupal stages. In *M. sexta*, the developmental delays caused by imaginal disc damage occur in the stages of development surrounding metamorphosis, when tissue size regulation is critical to ensure proper adult development. This is in contrast to *D. melanogaster*, when development appears particularly prolonged in the larval stage. The fact that *M. sexta* has

some shared and some unique responses with *D. melanogaster* suggests that it may be a strong complementary model to understanding the cellular mechanisms regulating these delays. Our results suggest that disruption of tissue development homeostasis in *M. sexta* through irradiation-induced imaginal disc damage may uncouple hormone-driven physiological milestones, presumably by attempting to prioritize tissue repair to ensure proper adult development. In particular, we now have a system to assess the role of JH independent of nutritional signals that define critical weight in irradiated larvae. It will be important to understand what cues are regulating development without altering growth in these damaged animals. The next steps are therefore to define the mechanisms that change critical weight and induce developmental delays.

Acknowledgements
We thank Iswar Hariharan for the use of his Faxitron machine at the University of California, Berkeley, and his willingness to welcome M.F. to his lab meetings; Adrian Halme for his insights and introduction to this research area; Annette Chan and the Cell and Molecular Imaging Center for overseeing use of the confocal microscopes; Sharon A. Chang for laboratory assistance of ecdysteroid measurements; and Michael Lin, Cleopa Omondi and Cheikh Njie for technical assistance with animals.

Competing interests
The authors declare no competing or financial interests.

Author contributions
Conceptualization: M.A.R., C.A.M., M.F.; Methodology: M.A.R., B.A., N.J.S., B.C.L., T.M., E.S.C., S.J.B., L.S.R., M.F.; Validation: M.A.R., B.A., N.J.S., B.C.L., J.A.Z., S.J.B., L.S.R., M.F.; Formal analysis: M.A.R., B.A., N.J.S., B.C.L., J.A.Z., E.S.C., M.F.; Investigation: M.A.R., B.A., N.J.S., B.C.L., J.A.Z., T.M., E.S.C., S.J.B., L.S.R., M.F.; Resources: M.F.; Data curation: M.A.R., B.C.L., S.J.B., M.F.; Writing - original draft: M.A.R., M.F.; Writing - review & editing: S.J.B., C.A.M.; Visualization: M.A.R., M.F.; Supervision: M.A.R., M.F.; Project administration: M.A.R., M.F.; Funding acquisition: C.A.M.

Funding
This work was supported by the National Institutes of Health [NIH 1SC2GM095428-01A1 to M.F., NIH 1SC3GM118218-01A1 to M.F.]; the National Science Foundation [NSF IOS-1257732 to E.S. Chang]; the CSU Program for Education & Research in Biotechnology [CSUperb Faculty-Student Collaborative Research Seed Grant to M.F.], the Computing for Life Sciences Award [SFSU-CCLI minigrant to M.F.]. SFSU Instructional Research Awards were awarded to B.A., B.C.L., L.S.R., and M.A.R. National Institutes of Health Fellowships were awarded as follows: NIH Bridges to the PhD [R25-GM048972 to B.A., J.A.Z., L.S.R. and M.A.R.]; NIH Research Training Initiative for Student Enhancement [R25-GM059298 to B.A., B.C.L. and N.J.S.]; NIH Maximizing Access to Research Careers [MARC T34-GM008574 to B.C.L., L.S.R. and N.J.S.]; NIH SFSU-CCSF Bridges to the Baccalaureate [5R25-GM050078 to L.S.R.]. A Genentech Dissertation Fellowship was awarded to M.A.R. A National Science Foundation Louis Stokes Alliances for Minority Participation Award [LSAMP HRD-0802628] was awarded to J.A.Z. Deposited in PMC for release after 12 months.

Supplementary information
Supplementary information available online at
http://jeb.biologists.org/lookup/doi/10.1242/jeb.200352.supplemental

References
Abuhagr, A. M., Blindert, J. L., Nimitkul, S., Zander, I. A., LaBere, S. M., Chang, S. A., MacLea, K. S., Chang, E. S. and Mykles, D. L. (2014). Molt regulation in green and red color morphs of the crab *Carcinus maenas*: gene expression of molt-inhibiting hormone signaling components. *J. Exp. Biol.* **217**, 796-808. doi:10.1242/jeb.093385

Arama, E. and Steller, H. (2006). Detection of apoptosis by terminal deoxynucleotidyl transferase-mediated dUTP nick-end labeling and acridine orange in *Drosophila* embryos and adult male gonads. *Nat. Prot.* **1**, 1725-1731. doi:10.1038/nprot.2006.235

Boulan, L., Andersen, D., Colombani, J., Boone, E. and Léopold, P. (2019). Inter-organ growth coordination is mediated by the Xrp1-Dilp8 axis in *Drosophila*. *Dev. Cell* **49**, 1-8. doi:10.1016/j.devcel.2019.03.016

Bourgin, R. C., Krumins, R. and Quastler, H. (1956). Radiation-induced delay of pupation in *Drosophila*. *Radiation Res.* **5**, 657. doi:10.2307/3570585

Bryant, P. J. (1971). Regeneration and duplication following operations *in situ* on the imaginal discs of *Drosophila melanogaster*. *Dev. Biol.* **26**, 637-651. doi:10.1016/0012-1606(71)90146-1

Bryant, P. J. and Fraser, S. E. (1988). Wound healing, cell communication, and DNA synthesis during imaginal disc regeneration in *Drosophila*. *Dev. Biol.* **127**, 197-208. doi:10.1016/0012-1606(88)90201-1

Bryant, P. J. and Simpson, P. (1984). Intrinsic and extrinsic control of growth in developing organs. *Quart. Rev. Biol.* **59**, 387-415. doi:10.1086/414040

Colombani, J., Andersen, D. S. and Léopold, P. (2012). Secreted peptide Dilp8 coordinates drosophila tissue growth with developmental timing. *Science* **336**, 582-585. doi:10.1126/science.1216689

Copenhaver, P. F. and Truman, J. W. (1982). The role of eclosion hormone in the larval ecdyses of *Manduca sexta*. *J. Insect Physiol.* **28**, 695-701. doi:10.1016/0022-1910(82)90148-2

Cymborowski, B., Bogus, M., Beckage, N. E., Williams, C. M. and Riddiford, L. M. (1982). Juvenile hormone titres and metabolism during starvation-induced supernumerary larval moulting of the tobacco hornworm, *Manduca sexta* L. *J. Insect Physiol.* **28**, 129-135. doi:10.1016/0022-1910(82)90120-2

D'Amico, L. J., Davidowitz, G. and Nijhout, H. F. (2001). The developmental and physiological basis of body size evolution in an insect. *Proc. Royal Soc. London B Biol. Sci.* **268**, 1589-1593. doi:10.1098/rspb.2001.1698

Davey, K. G. (2007). From insect ovaries to sheep red blood cells: a tale of two hormones. *J. Insect Physiol.* **53**, 1-10. doi:10.1016/j.jinsphys.2006.10.005

Davidowitz, G. (2016). Endocrine proxies can simplify endocrine complexity to enable evolutionary prediction. *Int. Comp. Biol.* **56**, 198-206. doi:10.1093/icb/icw021

Davidowitz, G., D'Amico, L. J. and Nijhout, H. F. (2003). Critical weight in the development of insect body size. *Evo. Dev.* **5**, 188-197. doi:10.1046/j.1525-142X.2003.03026.x

Davidowitz, G., Roff, D. and Nijhout, H. F. (2016). Synergism and antagonism of proximate mechanisms enable and constrain the response to simultaneous selection on body size and development time: an empirical test using experimental evolution. *Am. Nat.* **188**, 499-520. doi:10.1086/688653

Ely, M. J. and Jungreis, A. M. (1977). Radiation-Induced inhibition of eclosion in the tobacco hornworm, *Manduca sexta*. *Biol. Bull.* **152**, 169-181. doi:10.2307/1540557

Garelli, A., Gontijo, A. M., Miguela, V., Caparros, E. and Dominguez, M. (2012). Imaginal discs secrete Insulin-Like Peptide 8 to mediate plasticity of growth and maturation. *Science* **336**, 579-582. doi:10.1126/science.1216735

Hackney, J. F., Zolali-Meybodi, O. and Cherbas, P. (2012). Tissue damage disrupts developmental progression and ecdysteroid biosynthesis in *Drosophila*. *PLoS ONE* **7**, e49105. doi:10.1371/journal.pone.0049105

Halme, A., Cheng, M. and Hariharan, I. K. (2010). Retinoids regulate a developmental checkpoint for tissue regeneration in *Drosophila*. *Curr. Biol.* **20**, 458-463. doi:10.1016/j.cub.2010.01.038

Hatakoshi, M., Nakayama, I. and Riddiford, L. M. (1988). The induction of an imperfect supernumerary larval moult by juvenile hormone analogues in *Manduca sexta*. *J. Insect Physiol.* **34**, 373-378. doi:10.1016/0022-1910(88)90106-0

Hatem, N. E., Wang, Z., Nave, K. B., Koyama, T. and Suzuki, Y. (2015). The role of juvenile hormone and insulin/TOR signaling in the growth of *Manduca sexta*. *BMC Biol.* **13**, 44. doi:10.1186/s12915-015-0155-z

Helm, B. R. and Davidowitz, G. (2015). Evidence of a hemolymph-born factor that induces onset of maturation in *Manduca sexta* larvae. *J. Insect Physiol.* **78**, 78-86. doi:10.1016/j.jinsphys.2015.04.015

Jaszczak, J. S., Wolpe, J. B., Dao, A. Q. and Halme, A. (2015). Nitric oxide synthase regulates growth coordination during *Drosophila melanogaster* imaginal disc regeneration. *Genetics* **200**, 1219-1228. doi:10.1534/genetics.115.178053

Jones, G., Wozniak, M., Chu, Y. X., Dhar, S. and Jones, D. (2001). Juvenile hormone III-dependent conformational changes of the nuclear receptor ultraspiracle. *Insect Biochem. Mol. Biol.* **32**, 33-49. doi:10.1016/S0965-1748(01)00077-7

Kayukawa, T. and Shinoda, T. (2015). Functional characterization of two paralogous JH receptors, methoprene-tolerant 1 and 2, in the silkworm, *Bombyx mori* (Lepidoptera: Bombycidae). *App. Entomol. Zool.* **50**, 383-391. doi:10.1007/s13355-015-0345-8

Kayukawa, T., Murata, M., Kobayashi, I., Muramatsu, D., Okada, C., Uchino, K., Sezutsu, H., Kiuchi, M., Tamura, T., Hiruma, K. et al. (2014). Hormonal regulation and developmental role of Krüppel homolog 1, a repressor of metamorphosis, in the silkworm *Bombyx mori*. *Dev. Biol.* **388**, 48-56. doi:10.1016/j.ydbio.2014.01.022

Kingan, T. G. (1989). A competitive enzyme-linked immunosorbent assay: applications in the assay of peptides, steroids, and cyclic nucleotides. *Analyt. Biochem.* **183**, 283-289. doi:10.1016/0003-2697(89)90481-8

Koyama, T., Syropyatova, M. O. and Riddiford, L. M. (2008). Insulin/IGF signaling regulates the change in commitment in imaginal discs and primordia by overriding the effect of juvenile hormone. *Dev. Biol.* **324**, 258-265. doi:10.1016/j.ydbio.2008.09.017

Kunkel, J. G. (1977). Cockroach molting. II. The nature of regeneration-induced delay of molting hormone secretion. *Biol. Bull.* **153**, 145-162. doi:10.2307/1540698

Lee, S.-H., Oh, H.-W., Fang, Y., An, S.-B., Park, D.-S., Song, H.-H., Oh, S.-R., Kim, S.-Y., Kim, S., Kim, N. et al. (2015). Identification of plant compounds that disrupt

the insect juvenile hormone receptor complex. *Proc. Natl. Acad. Sci. USA* **112**, 1733-1738. doi:10.1073/pnas.1424386112

Livak, K. J. and Schmittgen, T. D. (2001). Analysis of relative gene expression data using real-time quantitative PCR and the $2-\Delta\Delta CT$ method. *Methods* **25**, 402-408. doi:10.1006/meth.2001.1262

Madhavan, K. and Schneiderman, H. (1969). Hormonal control of imaginal disc regeneration in *Galleria mellonella* (Lepidoptera). *Biol. Bull.* **137**, 321-331. doi:10.2307/1540104

Malá, J., Sehnal, F., Kumaran, A. K. and Granger, N. A. (1987). Effects of starvation, chilling, and injury on endocrine gland function in *Galleria mellonella*: environmental effects on endocrine gland function. *Arch. Insect Biochem. Physiol.* **4**, 113-128. doi:10.1002/arch.940040205

Minakuchi, C., Zhou, X. and Riddiford, L. M. (2007). Krüppel homolog 1 (Kr-h1) mediates juvenile hormone action during metamorphosis of *Drosophila melanogaster*. *Mech. Dev.* **125**, 91-105. doi:10.1016/j.mod.2007.10.002

Minakuchi, C., Namiki, T. and Shinoda, T. (2009). Krüppel homolog 1, an early juvenile hormone-response gene downstream of Methoprene-tolerant, mediates its anti-metamorphic action in the red flour beetle *Tribolium castaneum*. *Dev. Biol.* **325**, 341-350. doi:10.1016/j.ydbio.2008.10.016

Mirth, C., Truman, J. W. and Riddiford, L. M. (2005). The role of the prothoracic gland in determining critical weight for metamorphosis in *Drosophila melanogaster*. *Curr. Biol.* **15**, 1796-1807. doi:10.1016/j.cub.2005.09.017

Mirth, C. K., Tang, H. Y., Makohon-Moore, S. C., Salhadar, S., Gokhale, R. H., Warner, R. D., Koyama, T., Riddiford, L. M. and Shingleton, A. W. (2014). Juvenile hormone regulates body size and perturbs insulin signaling in *Drosophila*. *Proc. Natl. Acad. Sci. USA* **111**, 7018-7023. doi:10.1073/pnas.1313058111

Nijhout, H. F. (2015). Big or fast: two strategies in the developmental control of body size. *BMC Biol.* **13**, 57. doi:10.1186/s12915-015-0173-x

Nijhout, H. F. and Williams, C. M. (1974a). Control of moulting and metamorphosis in the tobacco hornworm, *Manduca sexta* (L.): growth of the last-instar larva and the decision to pupate. *J. Exp. Biol.* **61**, 481-491.

Nijhout, H. F. and Williams, C. M. (1974b). Control of moulting and metamorphosis in the tobacco hornworm, *Manduca sexta* (L.): cessation of juvenile hormone secretion as a trigger for pupation. *J. Exp. Biol.* **61**, 493-501.

Nijhout, H. F., Cinderella, M. and Grunert, L. W. (2014). The development of wing shape in Lepidoptera: mitotic density, not orientation, is the primary determinant of shape. *Evo. Dev.* **16**, 68-77. doi:10.1111/ede.12065

O'Brien, R. D. and Wolf, L. S. (1964). *Radiation, Radioactivity, and insects*. New York: Academic Press.

O'Farrell, A. F. and Stock, A. (1953). Regeneration and the moulting cycle in *Blattella germanica* L. I. Single regeneration initiated during the first instar. *Austrian J. Biol. Sci.* **6**, 485-500. doi:10.1071/BI9530485

O'Farrell, A. F. and Stock, A. (1954). Regeneration and the moulting cycle in *Blattella germanica* L. III. Successive regeneration of both metathoracic legs. *Austrian J. Biol. Sci.* **7**, 525-536. doi:10.1071/BI9540525

Pastor-Pareja, J. C., Wu, M. and Xu, T. (2008). An innate immune response of blood cells to tumors and tissue damage in *Drosophila*. *Dis. Model Mech.* **1**, 144-154. doi:10.1242/dmm.000950

Poodry, C. A. and Woods, D. F. (1990). Control of the developmental timer for *Drosophila* pupariation. *Roux's Arch. Dev. Biol.* **199**, 219-227. doi:10.1007/BF01682081

Riddiford, L. M., Curtis, A. T. and Kiguchi, K. (1979). Culture of the epidermis of the tobacco hornworm *Manduca sexta*. *Tissue Culture Association Manual* **5**, 975-985. doi:10.1007/BF00919715

RNeasy Mini Handbook (2012). *RNeasy Mini Handbook*. Germantown, MD, USA: QIAGEN.

Schubiger, G. (1971). Regeneration, duplication and transdetermination in fragments of the leg disc of *Drosophila melanogaster*. *Dev. Biol.* **26**, 277-295. doi:10.1016/0012-1606(71)90127-8

Simpson, P., Berreur, P. and Berreur-Bonnenfant, J. (1980). The initiation of pupariation in *Drosophila*: dependence on growth of the imaginal discs. *Dev.* **57**, 155-165. doi:10.1002/jez.1402100218

Smith, W., Lamattina, A. and Collins, M. (2014). Insulin signaling pathways in lepidopteran ecdysone secretion. *Front. Physiol.* **5**, 19. doi:10.3389/fphys.2014.00019

Stieper, B. C., Kupershtok, M., Driscoll, M. V. and Shingleton, A. W. (2008). Imaginal discs regulate developmental timing in *Drosophila melanogaster*. *Dev. Biol.* **321**, 18-26. doi:10.1016/j.ydbio.2008.05.556

Stock, A. and O'Farrell, A. F. (1954). Regeneration and the moulting cycle in *Blattella germanica* L. II. Simultaneous regeneration of both metathoracic legs. *Austrian J. Biol. Sci.* **7**, 302-307. doi:10.1071/BI9540302

Suzuki, Y., Koyama, T., Hiruma, K., Riddiford, L. M. and Truman, J. W. (2013). A molt timer is involved in the metamorphic molt in *Manduca sexta* larvae. *Proc. Natl. Acad. Sci. USA* **110**, 12518-12525. doi:10.1073/pnas.1311405110

Tanaka, K. and Truman, J. W. (2005). Development of the adult leg epidermis in *Manduca sexta*: contribution of different larval cell populations. *Dev. Genes Evo.* **215**, 78-89. doi:10.1007/s00427-004-0458-5

Trimmer, B. A. and Weeks, J. C. (1989). Effects of nicotinic and muscarinic agents on an identified motoneurone and its direct afferent inputs in larval *Manduca sexta*. *J. Exp. Biol.* **144**, 303-337.

Truman, J. W. and Riddiford, L. M. (1974). Physiology of insect rhythms: III. The temporal organization of the endocrine events underlying pupation of the tobacco hornworm. *J. Exp. Biol.* **60**, 371-382.

Truman, J. W., Hiruma, K., Allee, J. P., MacWhinnie, S. G. B., Champlin, D. T. and Riddiford, L. M. (2006). Juvenile hormone is required to couple imaginal disc formation with nutrition in insects. *Science* **312**, 1385-1388. doi:10.1126/science.1123652

Vallejo, D. M., Juarez-Carreño, S., Bolivar, J., Morante, J. and Dominguez, M. (2015). A brain circuit that synchronizes growth and maturation revealed through Dilp8 binding to Lgr3. *Science* **350**, aac6767. doi:10.1126/science.aac6767

Wells, C., Aparicio, K., Salmon, A., Zadel, A. and Fuse, M. (2006). Structure–activity relationship of ETH during ecdysis in the tobacco hornworm, *Manduca sexta*. *Peptides* **27**, 698-709. doi:10.1016/j.peptides.2005.08.001

Wilson, T. G. and Fabian, J. (1986). A *Drosophila melanogaster* mutant resistant to a chemical analog of juvenile hormone. *Dev. Biol.* **118**, 190-201. doi:10.1016/0012-1606(86)90087-4

Zhao, W.-L., Liu, C.-Y., Liu, W., Wang, D., Wang, J.-X. and Zhao, X.-F. (2014). Methoprene-tolerant 1 regulates gene transcription to maintain insect larval status. *J. Mol. Endocrinol.* **53**, 93-104. doi:10.1530/JME-14-0019

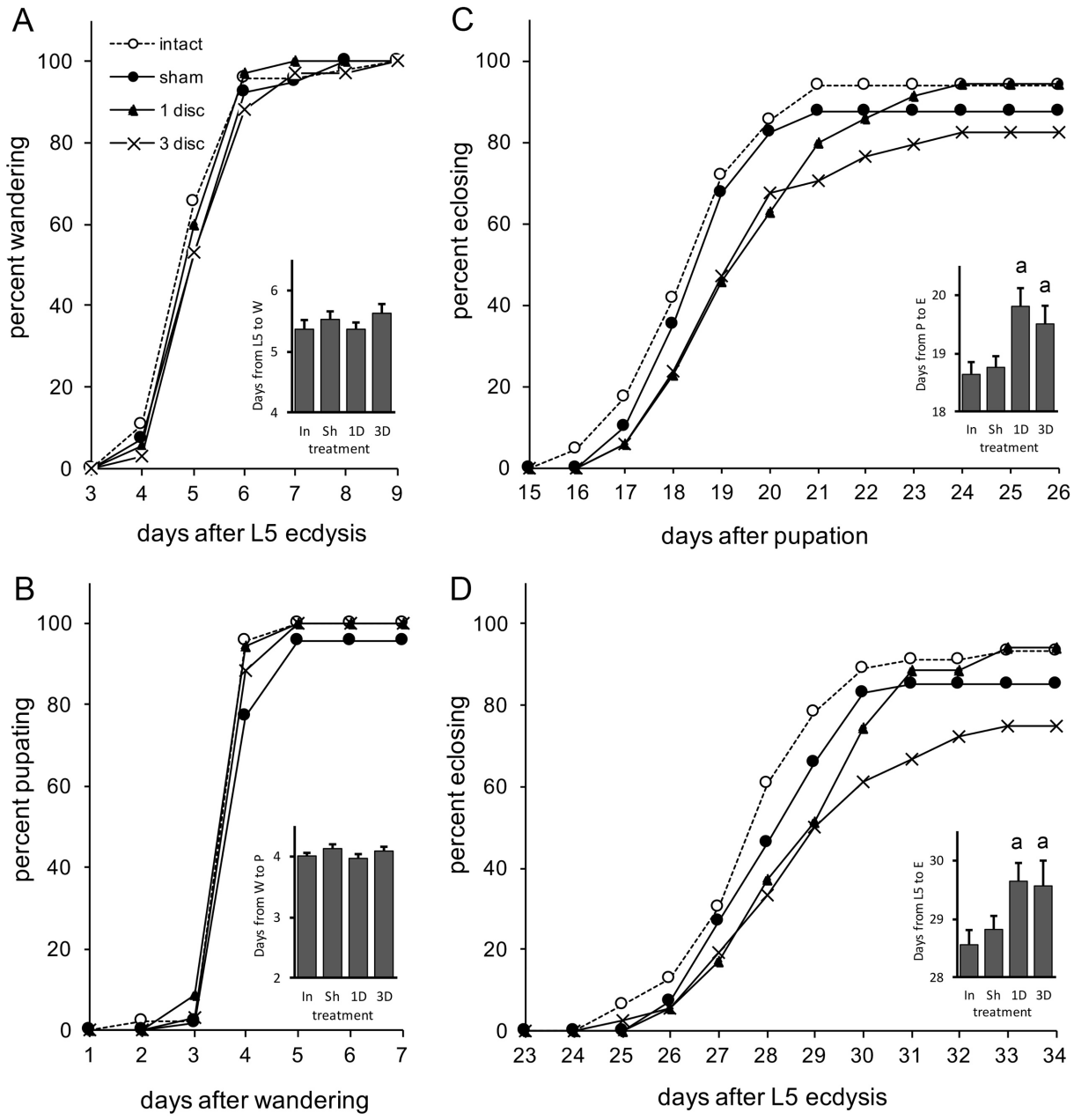

Journal of Experimental Biology • Supplementary information

Figure S1. Developmental timing is only moderately delayed after mechanical damage to wing imaginal discs. One wing (1D; n=36) or three wing (3D; n=37) imaginal discs were mechanically damaged in pharate fifth stage *M. sexta* larvae and were compared to intact (In; n=56) or 1 disc sham (Sh; n=41) controls. The percentage of animals were timed from (A) fracture to wandering, (B) wandering to pupation, (C) pupation to eclosion, and (D) fracture to eclosion. Insets represent average times with standard errors of the mean. Letters represent significant differences from each other, as assessed by one-way ANOVA with pairwise *t*-tests corrected by the Holm-Šidák method for multiple comparisons ($p<0.05$).

Journal of Experimental Biology • Supplementary information

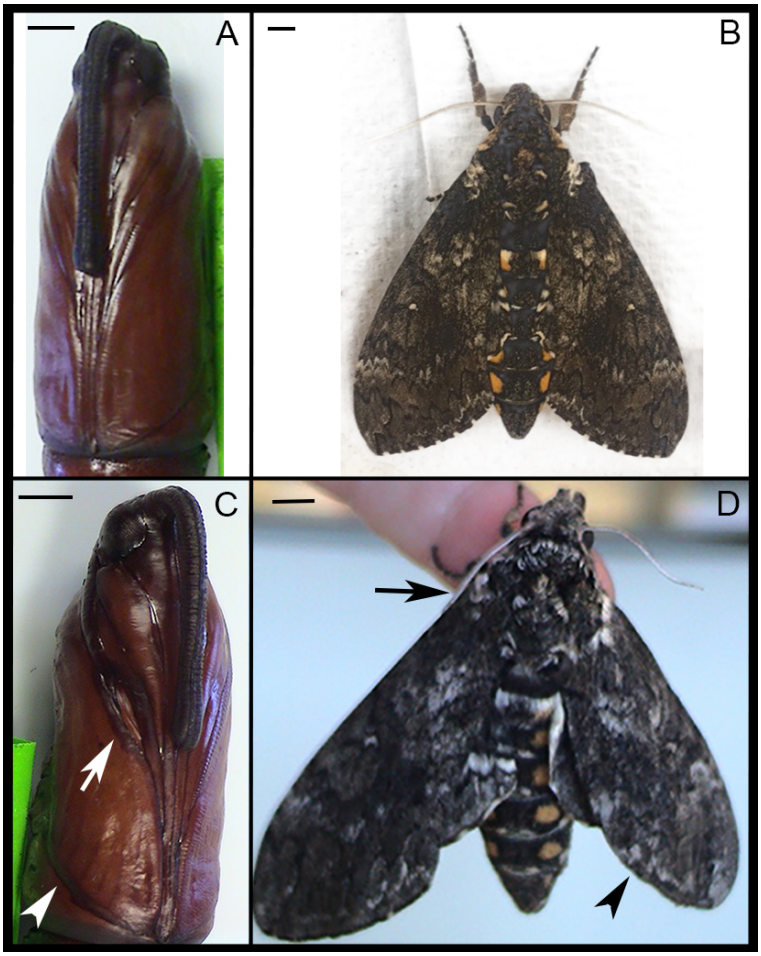

Figure S2. Pupal and adult phenotypes reveal damage after irradiation. Representative photos of pupae and adults showing sample morphological abnormalities after X-ray induced tissue damage. (A, B) healthy unirradiated pupa and adult, respectively, and (C, D) pupa and adult exposed to ~ 80 Gy irradiation with abnormalities. Arrows point to abnormal antennae and arrowheads point to abnormal wings. Note the sizes varied only for ease of representation, where the scale bars = 0.5 cm.

Journal of Experimental Biology • Supplementary information

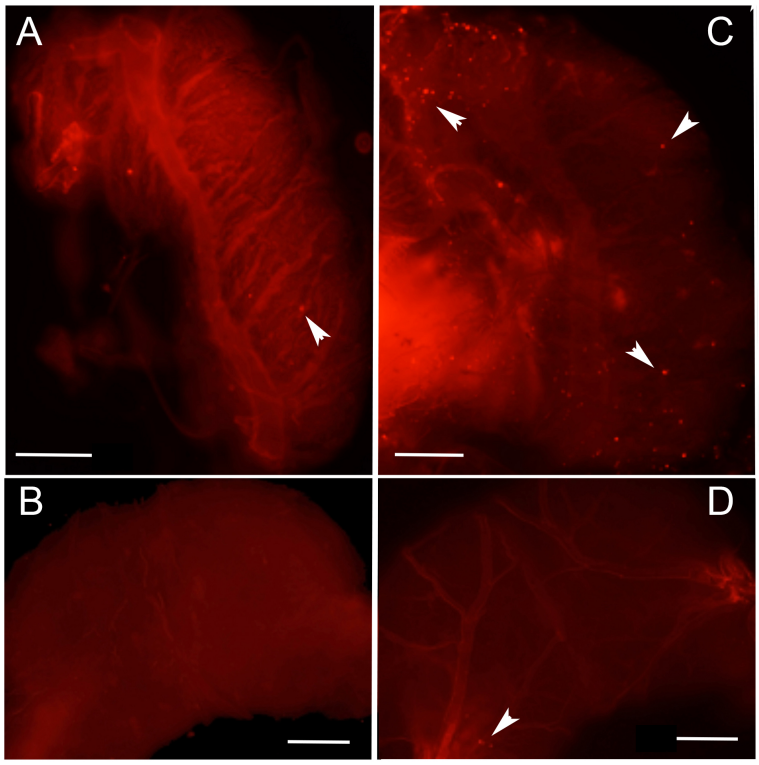

Figure S3. TUNEL stain is increased in wing imaginal discs but not brains after irradiation. Apoptotic cells in the imaginal disc of *M. sexta* imaged after TUNEL stain. Images reflect time points 12 h after irradiation at 60 Gy. White arrowheads indicate TUNEL stain in control forewing imaginal disc (A) and irradiated forewing imaginal disc (C) and brain (D). Control brains (B) typically had no stain. Scale bar represents 500 μm for (A, C), and 100 μm for (B, D).

Journal of Experimental Biology • Supplementary information

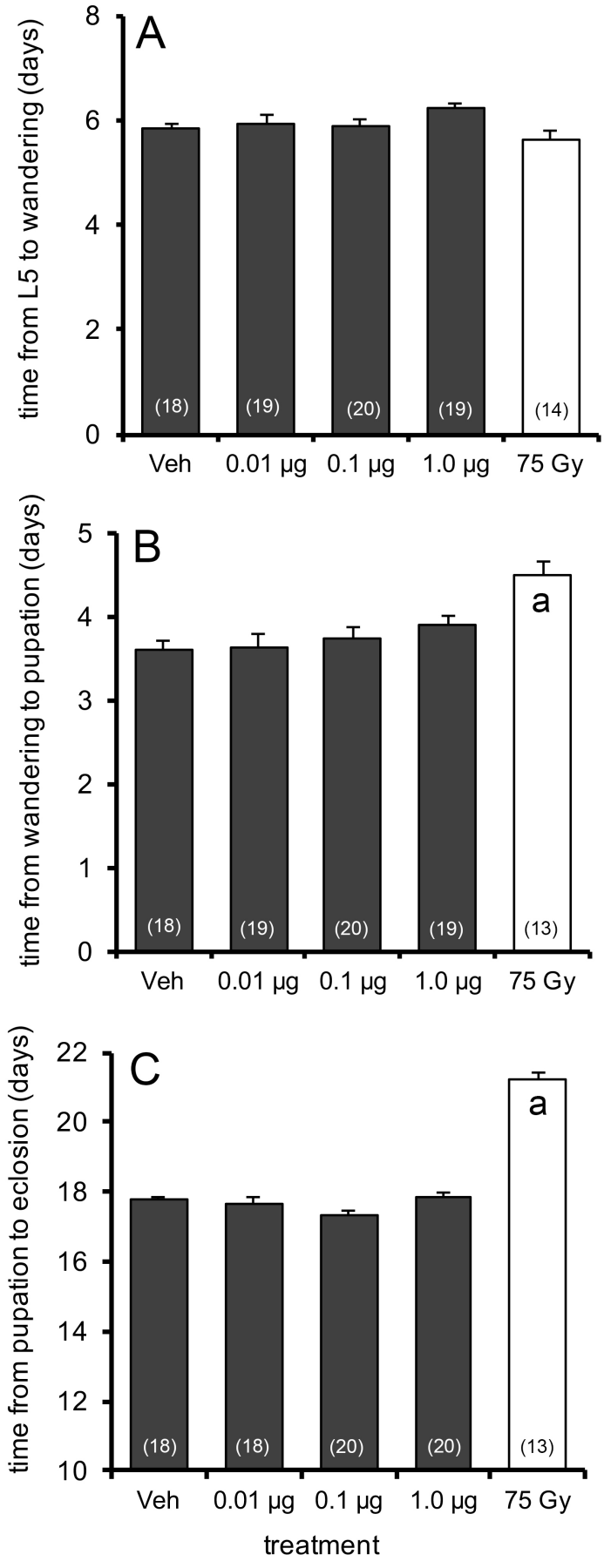

Journal of Experimental Biology • Supplementary information

Figure S4. Supplementation with a JH analog does not mimic the effects of irradiation. Healthy animals were supplemented with a JH analog, methoprene at 3 doses: 0.01, 0.1 and 1 μg animal^{-1} (grey bars), and compared to vehicle injections ("Veh") as well as vehicle-injected irradiated animals ("75 Gy"). Development was tracked for (A) the time to wander relative to 5th instar ecdysis, (B) the time to pupate relative to wandering, or (C) the time to eclose relative to pupation**.** Control larvae were irradiated at 75 Gy (white bar). Bars represent the average times with SEM. Sample sizes are noted within the bars. Letters represent significant differences from other groups within a developmental period, as assessed by one-way ANOVA with *post hoc* pairwise t-tests corrected by the Holm-Šidák method for multiple comparisons ($p<0.05$).

Journal of Experimental Biology • Supplementary information

Table S1. NCBI tBlastn query search of *D. melanogaster* DILP8 protein sequence in a variety of insect genomes. Several related *Drosophila* species, several holometabolous insect genomes and two outgroups (Blattodea & Orthoptera) were assessed for the presence of a DILP8-like protein. *M. sexta* BLAST query was performed additionally using NAL i5k database, which attributed any sequence matches to background noise (high E-value). 'None' denotes no alignments returned. Query result shows high sequence similarity in local alignment (Total score) for only Diptera species, with only *Drosophila* showing high overlap of DILP8 sequence to the subject sequence (Query coverage), and the significance of the alignment (E-value close to zero value). Hits returned with high E-value score suggests total score may be random similarities.

Species	Total Score	Query Cover	E-value
Diptera			
Drosophila yakuba (Meigen)	282	100%	3e-97
Drosophila sechellia (Tsacas and Baechli)	306	97%	1e-108
Drosophila simulans (Sturtevant)	310	100%	5e-106
Drosophila erecta (Tsacas and Lachaise)	295	100%	2e-102
Drosophila ananassae (Doleschall)	258	100%	8e-88
Drosophila grimshawi (Oldenberg)	178	100%	9e-59
Aedes aegypti (Linnaeus)	28.1	21%	8.1
Anopheles gambiae (Giles)	25	8%	8.2
Lepidoptera			
Manduca sexta (Linnaeus)	31.6	29%	2.4
Bombyx mori (Linnaeus)	None	None	None
Bombyx mandarina (Moore)	None	None	None
Coleoptera			
Tribolium castaneum (Herbst)	None	None	None
Blattodea**			
Periplaneta americana (Linnaeus)	None	None	None
Orthoptera**			
Schistocerca americana (Drury)	None	None	None

** outgroups